行政院國家科學委員會專題研究計畫 成果報告

震動夯實造成之土壤應力及密度變化(II)
研究成果報告(精簡版)

計 畫 類 別 ：個別型
計 畫 編 號 ：NSC 98-2221-E-009-135-
執 行 期 間 ：98 年 08 月 01 日至 99 年 07 月 31 日
執 行 單 位 ：國立交通大學土木工程學系（所）

計 畫 主 持 人：方永壽

計畫參與人員：碩士班研究生-兼任助理人員：林卓民
碩士班研究生-兼任助理人員：陳威廷
碩士班研究生-兼任助理人員：徐育芬

報 告 附 件 ：出席國際會議研究心得報告及發表論文

處 理 方 式 ：本計畫可公開查詢

中 華 民 國 99 年 08 月 11 日

行政院國家科學委員會補助專題研究計畫 ■ 成 果 報 告 □期中進度報告

震動夯實造成之土壤應力及密度變化 (II)

計畫類別：■ 個別型計畫　　□ 整合型計畫
計畫編號：NSC 98－2221－E－009－135－
執行期間：98 年 08 月 01 日至 99 年 07 月 31 日

計畫主持人： 方永壽 教授
計畫參與人員： 陳威廷 碩士班研究生

成果報告類型(依經費核定清單規定繳交)：□精簡報告　■完整報告

本成果報告包括以下應繳交之附件：
□赴國外出差或研習心得報告一份
□赴大陸地區出差或研習心得報告一份
■出席國際學術會議心得報告及發表之論文各一份
□國際合作研究計畫國外研究報告書一份

處理方式：除產學合作研究計畫、提升產業技術及人才培育研究計畫、列管計畫及下列情形者外，得立即公開查詢
□涉及專利或其他智慧財產權，□一年□二年後可公開查詢

執行單位： 國立交通大學土木工程學系

中　華　民　國　99　年　8　月　10　日

震動夯實造成之土壤應力及密度變化 (II)

摘要

本研究探討條形振動夯實造成砂土密度和土壓力的變化。本研究以氣乾之渥太華砂為回填土，回填土高 1.5 公尺。回填土初始相對密度為 34%。為了在實驗室模擬雙向平面應變的情況，本研究採用塑膠膜潤滑層來降低砂土和填砂槽側牆間的摩擦力。根據實驗結果，獲得以下幾項結論：

1. 對於疏鬆砂土，土體內的垂直土壓力和水平土壓力可分別以 $\sigma_v = \gamma z$ 和 Jaky 公式來進行合理的估算。
2. 隨著夯實機夯實趟數的增加，條形夯實區之地表沉陷量隨之增大。地表沉陷量和夯實趟數之間的關係可以用雙曲線的模式來模擬。
3. 砂土的相對密度變化等高線範圍，會隨著夯實趟數增加而擴大。
4. 垂直土壓力變化量的等高線近似於同心圓的形狀，而殘餘垂直土壓力 $\Delta\sigma_v$ 會由圓心區域向外逐漸減少。土體內最大 $\Delta\sigma_v$ 值會隨著夯實趟數增加而增大。
5. 在夯實機夯實 1 和 2 趟後，殘餘水平土壓力 $\Delta\sigma_h$ 的等高線會形成兩個較高的應力區，水平土壓力變化量會由中心區域逐漸減少。然而在夯實機夯實 4 和 8 趟後，殘餘水平土壓力的等高線則近似於一個同心圓的形狀。夯實影響的區域 ($\Delta\sigma_h$ = 0.2 kN/m^2 應力等高線) 深度會隨著夯實能量增加而增大。
6. 在夯實一趟後，土壤所受夯實影響的機制可以用基礎下方土壤之局部剪力破壞的情況來解釋。然而，當夯實趟數增加到 8 趟後，被夯實土壤之機制可用方形鋼樁以振動打樁機貫入砂質地盤的情況來模擬。

關鍵字： 砂土、模型試驗、夯實、沉陷、相對密度、土壓力

Change of Soil Stress and Density due to Vibratory Compaction (II)

Abstract

This report studies the variation of soil density and earth pressure due to the strip compaction with a vibratory compactor. In this study, dry Ottawa sand was used as backfill material, and the height of backfill was 1.5 m. The initial relative density of the backfill was 34 %. To simulate a 2-way plane strain condition in the laboratory, the friction between the soil and sidewalls of the soil bin was reduced as much as possible. Based on the test results, the following conclusions can be drawn.

1. For loose sand, the vertical and horizontal earth pressure in the soil mass could be properly estimated with the equation $\sigma_v = \gamma z$ and Jaky's equation, respectively.
2. The surface settlement increased with the increasing number of passes of the compactor. The relationship between the surface settlement and the number of passes of the compactor could be modeled by the hyperbolic model.
3. After compaction, the range of contours of relative density (D_r = 36 %) became larger with increasing number of passes.
4. The contours of $\Delta\sigma_v$ were analogous to concentric circles, and the $\Delta\sigma_v$ would decrease gradually from the central region. The vertical stress increment $\Delta\sigma_v$ increased with increasing number of passages of the compactor.
5. The contours of $\Delta\sigma_h$ formed two circles of high stresses and $\Delta\sigma_h$ decreased gradually from the center region after the first and the second passes of compactor. The contours of $\Delta\sigma_h$ were analogous to concentric circles after 4 and 8 passes of the compactor. The depth of the compaction-induced zone increased with increasing compaction energy input.
6. Based on the test results, the mechanism of soils after the first pass of the compactor could be explained by local shear failure. However, the mechanism of soils after 8 passes of the compactor could be simulated by a steel square pile driven in sand with a vibratory hammer.

Keywords: sand, model test, compaction, settlement, relative density, earth pressure

Table of Contents

1. INTRODUCTION

In the construction of highway embankments, earth dams, and many other engineering structures, engineers will compact loose soils to increase their unit weights. The objective of the compaction operation is to improve the engineering properties of soil such as increasing the fill bearing capacity or reducing settlement. In various methods of compaction, vibratory compactions are used mostly for the densification of granular soils as shown in Fig. 1.

Before compaction, the vertical earth pressure is calculated by the equation $\sigma_v = \gamma z$, and the horizontal earth pressure is estimated with Jaky's formula. Many researchers had conducted studies regarding soil compaction, however most of their investigating were focused on compaction-induced stresses. It should be mentioned that the effects of compaction on a soil mass are not limited to stress change only. This study discusses the compaction-induced effects on a loose sandy soil which includes: (1) the surface settlement; (2) the change of relative density; (3) the change of vertical stresses; and (3) the change of horizontal stresses in the soil mass. Based on the experimental evidence, the mechanism of soil behavior under compaction is proposed.

1.1 Objective of Study

Compaction is a particular kind of soil stabilization methods and it is one of the oldest methods for improving existing soil or man-placed fills. To analyze the residual lateral earth pressure induced by soil compaction, several methods of analysis have been proposed by Rowe (1954), Broms (1971), Ingold (1979), Duncan and Seed (1986), Peck and Mesri (1987) and other researchers. However, little information regarding the mechanism of the compacted soil has been reported. From a practical point of view, this study simulates the strip compaction with a vibratory compactor on the surface of a loose granular soil in the field. The tests results include the change of soil density and the change of stress in the soil mass due to compaction. Based on the test data, the mechanism of the compacted soil due to the strip compaction on the surface of a sandy soil mass is proposed. All experiments mentioned in this study were conducted in the National Chiao Tung University (NCTU) non-yielding retaining wall facility. The horizontal and vertical stresses were measured with the soil pressure transducers (SPTs) which were embedded in the backfill.

Fig. 1. Compaction of Soil with Vibratory Compactor

2. LITERATURE REVIEW

Mesri and Hayat (1993) reported that Jaky (1944) established a relationship between K_o and maximum effective angle of internal friction ϕ by analyzing a talus of granular soil freestanding at the angle of repose. Jaky (1944) supposed that the angle of repose is analogous to the angle of internal friction ϕ. This is reasonable for sediment, normally consolidated material. Jaky (1944) reasoned that the sand cone OAD in Fig. 2 is in a state of equilibrium and its surface and inner points are motionless. The horizontal pressure acting on the vertical plane OC is the earth pressure at-rest. Slide planes exist in the inclined sand mass. However, as OC is a line of symmetry, shear stresses can not develop on it. Hence OC is a principal stress trajectory. Based on the equations of equilibrium, Jaky expressed the coefficient of earth pressure at-rest K_o with the angle of internal friction, ϕ:

$$K_o = (1 - \sin\phi)\frac{1 + \frac{2}{3}\sin\phi}{1 + \sin\phi} \tag{1}$$

In 1948, Jaky presented a modified simple expression given by Eq. 2

$$K_o = 1 - \sin\phi \tag{2}$$

Duncan and Seed (1986) presented an analytical procedure for evaluation of peak and residual compaction-induced stresses either in the free field or adjacent to vertical, non-deflecting soil-structure interfaces. This procedure employs a hysteretic K_o -loading model shown in Fig. 3 The model is adapted to incremental analytical methods for the evaluation of peak and residual earth pressures resulting from the placement and compaction of soil. When the surcharge is applied on the soil surface, it will increase the vertical stress and the horizontal stress. In Fig. 3, as the virgin loading is applied on the soil, both σ_v and σ_h increase along the K_o -line (K_o = *1-sin*ϕ). Nevertheless, when the surcharge is removed, σ_v and σ_h would decrease along the virgin unloading path. As virgin reloading was applied again, the increment of earth pressure is less than that induced by the first virgin loading.

The hysteretic model may be applied to the analysis of compaction as represented by a transient, moving surface load of finite lateral extent by directly modeling loading due to increased overburden as an increase in vertical effective stress ($\Delta\sigma'_v$). To model compaction loading in terms of the peak virgin, compaction-induced horizontal stress increase ($\Delta\sigma'_{h,vc,p}$) is defined as the horizontal effective stress which would be induced by the most critical positioning of the compactor. The $\Delta\sigma'_{h,vc,p}$ could be evaluated by the simple elastic analysis if the soil had been previous uncompacted (if the soil had no "lock-in" residual stresses due to previous compaction). While the hysteretic model is applied to the analysis of compaction loading cycle, the $\Delta\sigma'_{h,vc,p}$ should be transformed to an equivalent peak vertical load increment ($\Delta\sigma'_{v,e,p}$) calculated as

$$\Delta\sigma'_{v,e,p} = \frac{\Delta\sigma'_{h,vc,p}}{K_o} \quad (3)$$

It is important to note the peak compaction loading must be based on directly calculated lateral stress increase rather than directly calculated peak vertical stress increase multiplied by K_o, K_a or some other coefficient. Seed and Duncan (1983) concluded that either in the free field, or at or near vertical, non-deflecting soil/structure interfaces, $\Delta\sigma'_{h,vc,p}$ resulting from surface compaction loading can be calculated directly by simple elastic analysis. The parameter of Poisson's ratio, ν for surface compaction loading may be chosen according to the empirically derived relationship

$$\nu = \nu_o + \frac{1}{2}(0.5 - \nu_o) \quad (4)$$

where $\nu_o = \frac{K_o}{1 + K_o}$

In the field, the factors affecting compaction include the thickness of lift, the intensity of pressure applied by the compacting equipment, and the area over which the pressure is applied. During compaction, the dry unit weight of soil is affected by the number of roller passes. Johnson and Sallberg (1960) used 84.5 kN (19 kip) three-wheel roller to compact a silty clay in 229 mm (9 in) loose layers at different moisture contents. The test results show the growth curve that indicated the dry unit weight of a soil at a given moisture content increases to a certain point with the number of roller passes in Fig. 4.

In Fig. 5, D'Appolonia et al. (1969) reported the distribution of the unit weight of soil with depth for a poorly graded dune sand, for which compaction was achieved by a vibratory drum roller. Vibration was produced by mounting an eccentric weight on a single rotating shaft within the drum cylinder. The weight of the roller used for this compaction was 55.6 kN (12.5 kip), and the drum diameter was 1.19 m (47 in). The lifts were kept at 2.44m (8 ft). The dry unit weight of compacted soil increased with the number of roller passes. However, the rate of increase in unit weight gradually decreases after about 15 passes. The dry unit weight and hence the relative density D_r reached maximum values at a depth of about 0.5 m (1.5 ft) and gradually decreased at lesser depths. This decrease occurs because of the lack of confining pressure toward the surface.

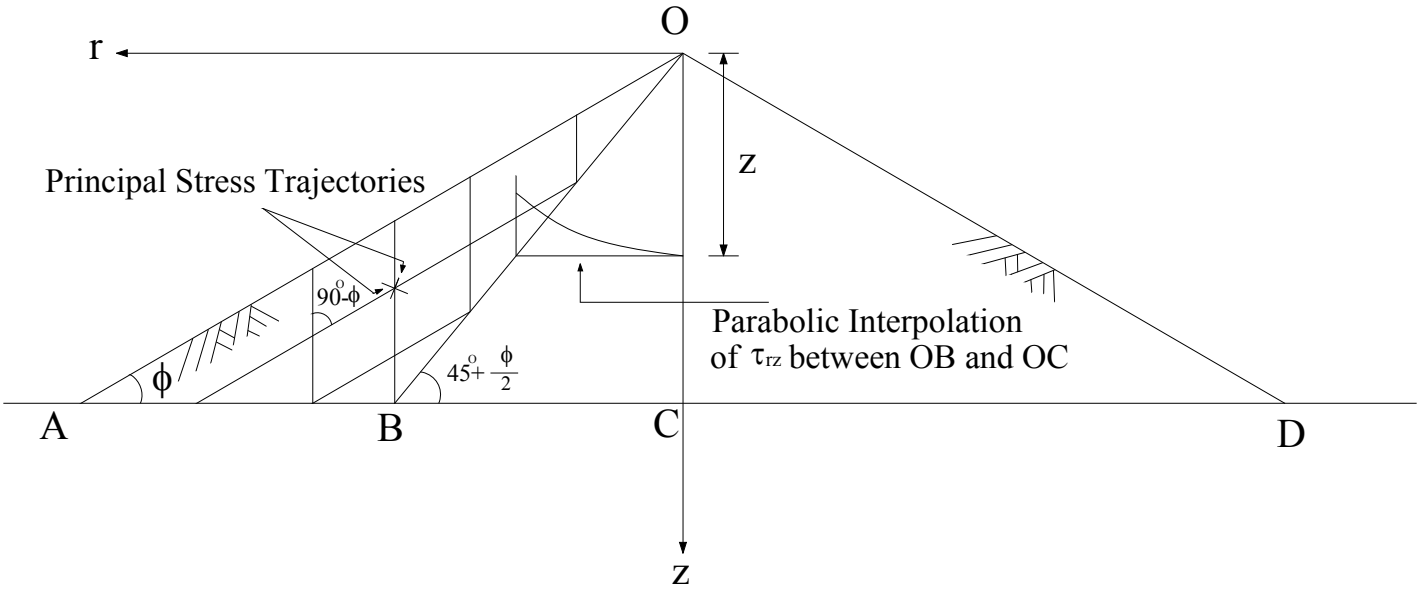

Fig. 2. Jaky's Formulation of the Relationship between K_o on OC and ϕ Mobilized in OAB (after Mesri and Hayat, 1993)

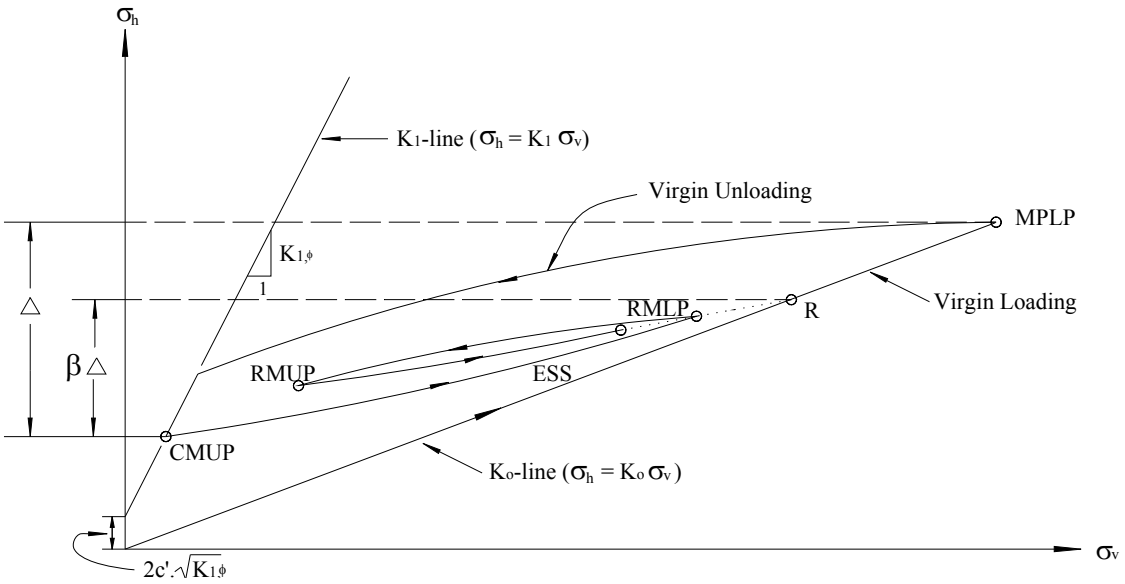

Fig. 3. Basic Components of Hysteretic K_o-Loading/Unloading Model (after Duncan and Seed, 1986)

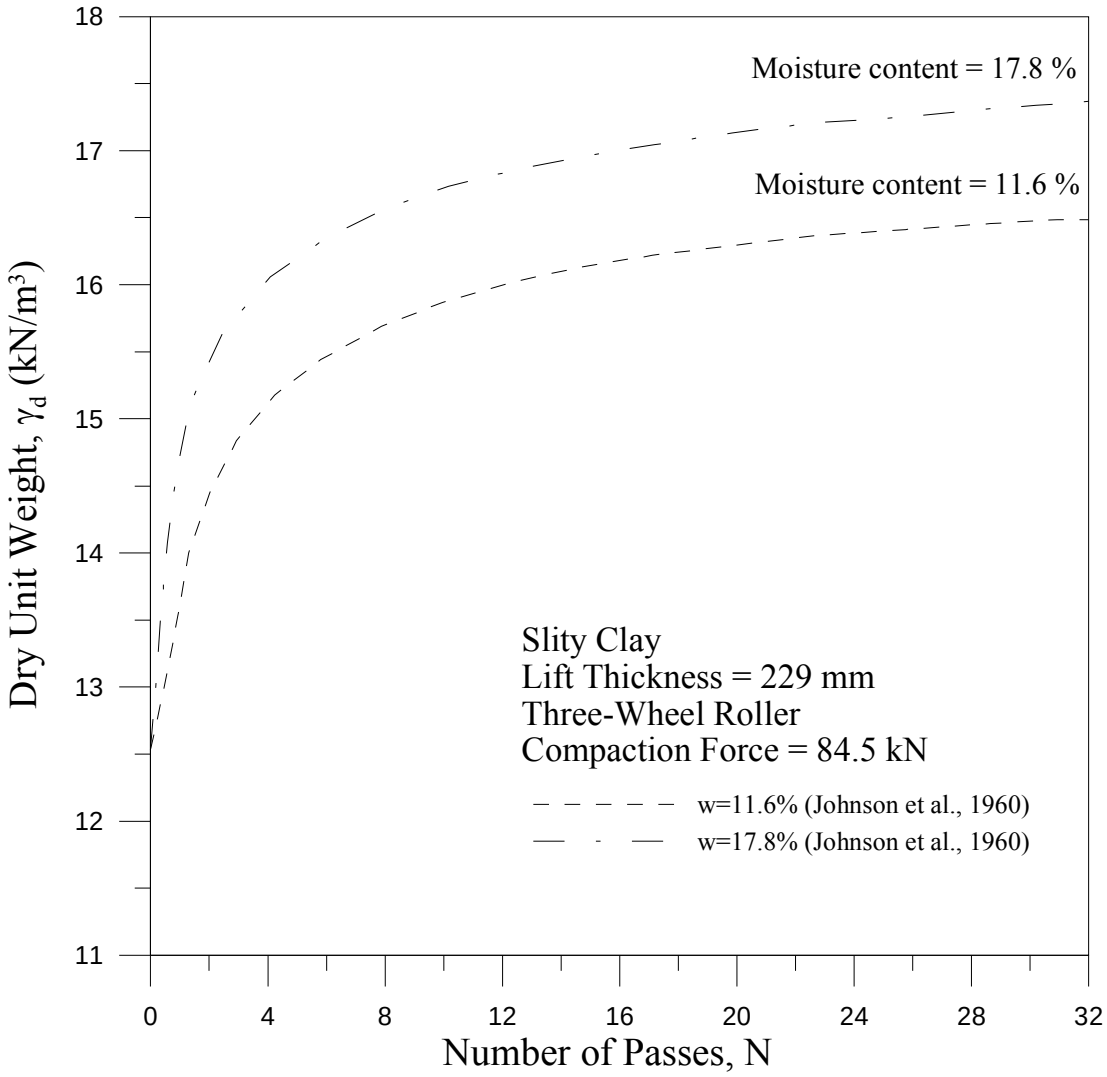

Fig. 4. Growth Curves for a Silty Clay – Relationship between Dry Unit Weight and Number of Passes of Three-Wheel Roller Compactor
(after Johnson and Sallberg, 1960)

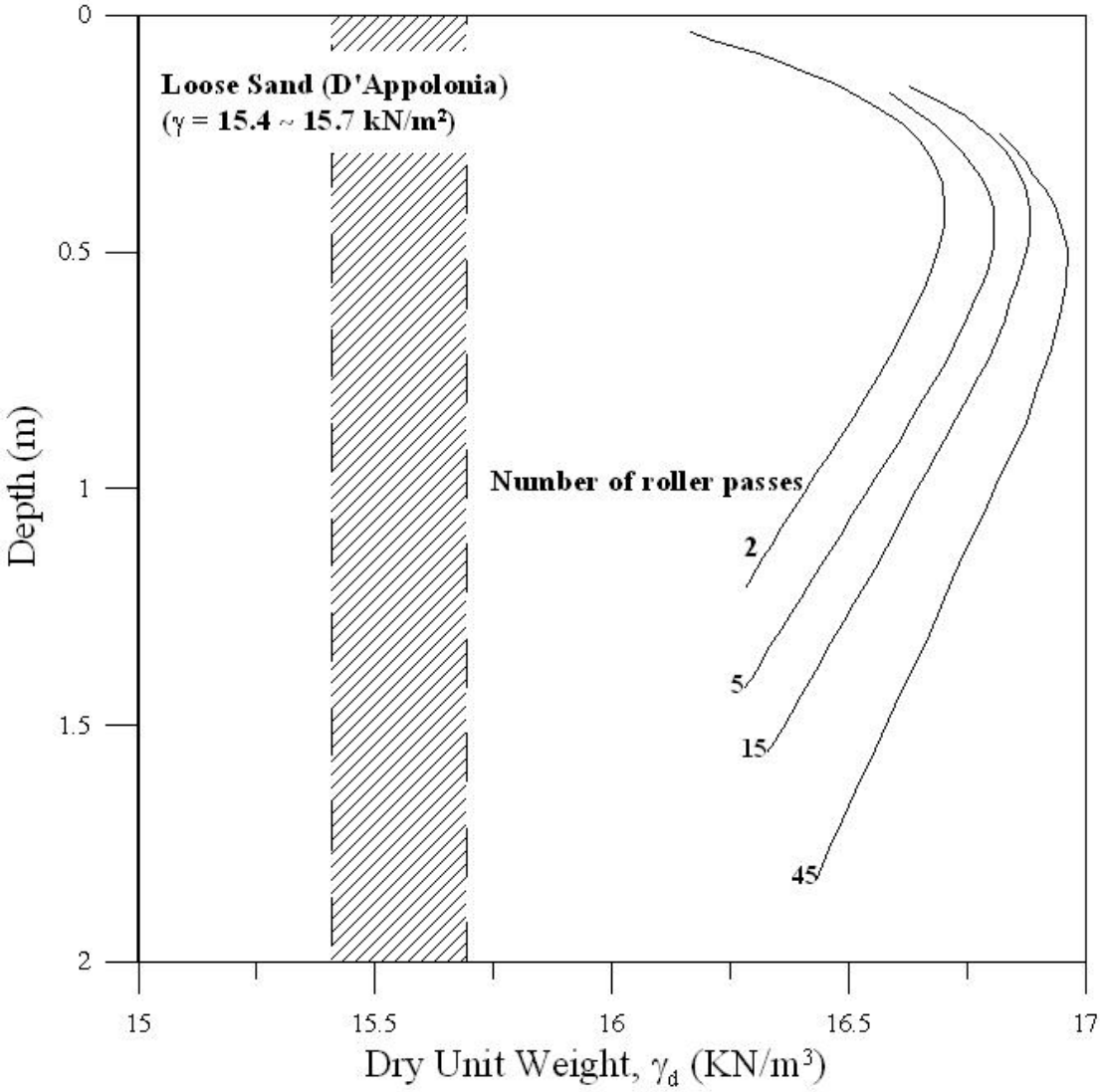

Fig. 5. Vibratory compaction of a sand - variation of dry unit weight with number of roller passes; thickness of lift = 2.45 m (after D'Appolonia, et al., 1969)

3. EXPERIMENTAL APPARATUS

To investigate the effects of vibratory compaction on the vertical and horizontal stresses in a cohesionless soil mass, the instrumented non-yielding model retaining wall facility at National Chiao Tung University (NCTU) was used. This chapter introduces the NCTU non-yielding retaining wall facilities and the vibratory compactor used to densify the loose backfill. The NCTU non-yielding retaining wall facilities consist of three components: (1) the soil bin, (2) soil pressure transducers, and (3) the data acquisition system (Chen and Fang, 2002). The details of the foregoing apparatuses are described in the following sections.

3.1 Soil Bin

To simulate a plan strain condition for model test, the soil bin is designed to minimize the lateral deflection of sidewalls. In Fig. 6, the soil bin was fabricated of steel plates with inside dimensions of 1500 mm × 1500 mm × 1600 mm. The soil bin was divided into two parts to discuss in the following section: (1) model wall, and (2) sidewall and end wall.

The model wall shown in Fig. 6 is 1500 mm-wide and 1600 mm-high, and 45 mm-thick. To achieve at-rest condition, the wall material should be nearly rigid. It is hoped that the deformation of the wall could be neglected with the application of earth pressure. As indicated in Fig. 6, twenty-four 20 mm-thick steel columns were welded to the four sidewalls to reduce any lateral deformation during loading. In addition, twelve C-shaped steel beams were also welded horizontally around the box to further increase the stiffness of the box.

Assuming a 1.5 m-thick cohesionless backfill with a unit weight γ = 17.1 kN/m^3, and an internal friction angle $\phi = 41^{\circ}$ was pluviated into the box. A 45 mm-thick solid steel plate with a Young's modulus of 210 GPa was chosen as the wall material. The estimated deflection of the model wall would be only 1.22×10^{-3} mm. Therefore, it can be concluded that the lateral movement of the model wall is negligible and an at-rest condition can be achieved.

The end-wall and sidewalls of the soil bin were made of 35 mm-thick steel plates. Outside the steel walls, vertical steel columns and horizontal steel beams were welded to increase the stiffness of the end-wall and sidewalls. If the soil bin was filled with dense sand, the estimated maximum deflection of the sidewall would be 1.86×10^{-3} mm. From a practical point of view, the deflection of the four walls around the soil bin can be neglected.

3.2 Soil Pressure Transducers

To investigate the distribution of stress in the backfill, a series of soil pressure transducers (Kyowa BE-2KCM17, capacity = 98.1 kN/m^2) as shown in Fig. 7 was used. The transducers were buried in the soil mass to measure the variation of vertical and horizontal earth pressure during the filling and compaction process. The five radial extensions projected from the transducer are used to prevent possible rotation of the transducer due to filling and compaction. The effective diameter of the transducer is 22 mm and its thickness is 6 mm.

3.3 Data Acquisition System

A data acquisition system was used to collect and store the considerable amount of data generated during the tests. The data acquisition system is composed of the following four parts: (1) dynamic strain amplifiers (Kyowa: DPM601A and DPM711B); (2) AD/DA card (NI

BNC-2090); and (3) Personal Computer. The analog signals from the sensors were filtered and amplified by the dynamic strain amplifiers. Then, the analog experimental data were digitized by an A/D-D/A card. The digital signals were then transmitted to the personal computer for storage and analysis.

3.4 Vibratory Soil Compactor

To simulate compaction of backfill in the field, the vibratory compactor shown in Fig. 8 was made by attaching an eccentric motor (Mikasa Sangyo, KJ75-2P) to a 0.225 m × 0.225 m steel plate. The eccentric force can be controlled by adjusting the number of eccentric steel plates attached to the rotating shaft of motor. For this study, a total of sixteen eccentric plates (8+8) were used. The detailed information regarding the eccentric motor is listed in Table 1.The dynamic vertical force F_d measured with a load cell placed under the base plate of the vibratory compactor with 16 eccentric plate, the corresponding F_d = 1.648 kN. With the static mass of the compactor (w = mg = 0.119 kN), the cyclic vertical force (static + dynamic) was 1.767 kN. The measured frequency of vibration was 44 Hz. Assuming the distribution of contact pressure between the base plate (0.225 m × 0.225 m) and soil is uniform, the cyclic normal stress σ_{cyc} applied on the surface of soil would be 34.9 kN/m^2 (5.06 psi). It should be mentioned that the distribution of contact pressure between the foundation and soil varies with the stiffness of the footing. If the footing is perfectly rigid, the static contact pressure on the footing increases from zero at the edge to a maximum at the center.

Table 1. Technical Information of the Eccentric Motor

Manufacture	Mikasa
Type	KJ75-2P
Power (Watt)	75
Voltage (Volt)	220
Frequency (Hz)	50/60
Vibration per Minute	3000/3600
Mass (kg)	6.2

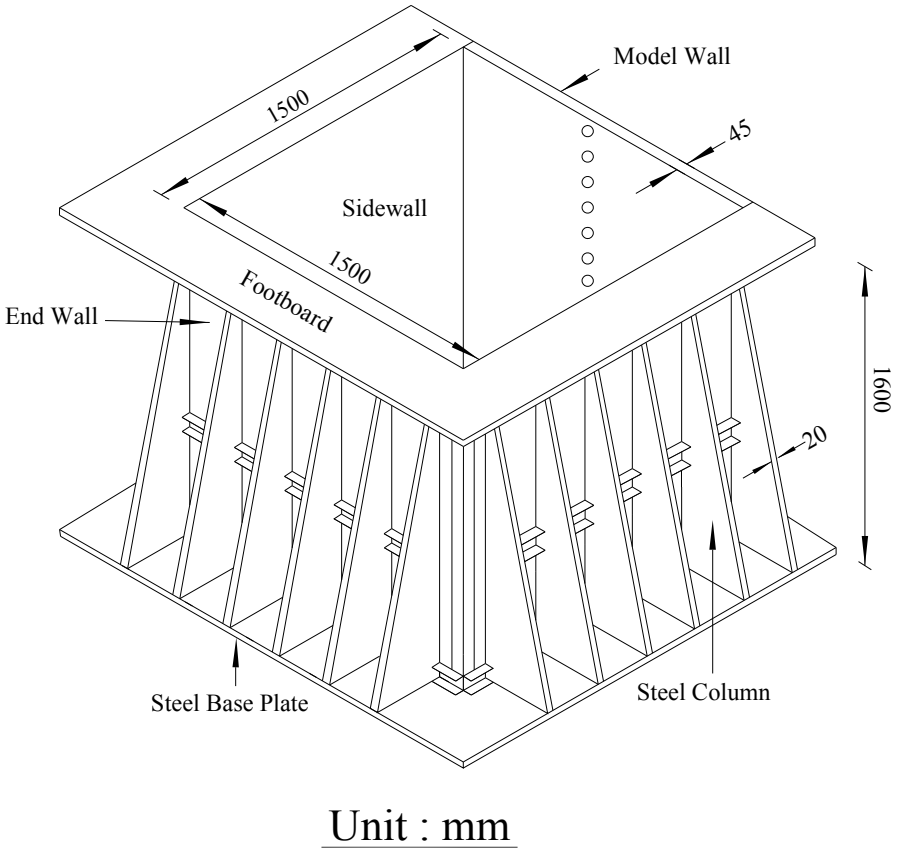

Fig. 6. NCTU Non-Yielding Retaining-Wall Facility (after Chen, 2002)

Fig. 7. Soil-Pressure Transducer (Kyowa BE-2KCM17) (after Chen, 2002)

Fig. 8. Vibratory Soil Compactor

4. BACKFILL CHARACTERISTICS

4.1 Backfill Properties

Air-dry Ottawa silica sand (ASTM C-778) was used as the backfill material in all experiments. Physical properties of the soil are summarized in Table 2. Grain-size distribution of the backfill is shown in Fig. 9.

To establish the relationship between unit weight of backfill γ and its internal friction angle ϕ, direct shear tests have been conducted. The shear box used has a square (60 mm $\times$ 60 mm) cross-section, and its arrangement is shown in Fig. 10. Before shearing, Ottawa sand was air-pluviated into the shear box and then compacted to the desired density.

Chang (2000) established the relationship between the internal friction angle ϕ and unit weight γ of Ottawa sand. It is obvious from the figure that soil strength increases with increasing soil density. For the air-pluviated backfill, the empirical relationship between soil unit weight γ and ϕ angle can be formulated as follows

$$\phi = 6.43\,\gamma - 68.99 \qquad (5)$$

where

ϕ = angle of internal friction of soil (degree)

γ = unit weight of soil (kN/m^3)

Eq. (5) is applicable for $\gamma = 15.45 \sim 17.4$ kN/m^3 only.

4.2 Reduction of Wall Friction

To constitute a plane strain condition for model wall tests, the shear stress between the backfill and wall should be minimized to nearly frictionless. To reduce the friction between wall and backfill, a lubrication layer fabricated with plastic sheets was furnished for all experiments. Two types of plastic sheeting, one thick and two thin plastic sheets were adopted to reduce the interface friction. All plastic sheets were hung vertically on four walls before the backfill was placed.

The variation of friction angle δ_w as a function of the normal stress σ_n for the plastic sheet method (1 thick + 2 thin sheeting) used in this study. The measured friction angle with this method is about 7.5°. This constancy is an important advantage in establishing the input soil properties for analytical models that might be used to analyze the experimental results. For all experiments in this paper, the lubrication layer wall applied on four walls. The plastic sheets not only can help to reduce the friction angle between the wall and the backfill. The plastic sheets can also help to reduce the reflection of elastic waves transmitted to the soil-wall boundaries during compaction.

Table 2. Properties of Ottawa Sand (after Hou, 2006)

Shape	*Rounded*
e_{max}	*0.76*
e_{min}	*0.50*
G_s	*2.65*
D_{60} *(mm)*	*0.32*
D_{10} *(mm)*	*0.21*
C_u	*1.78*

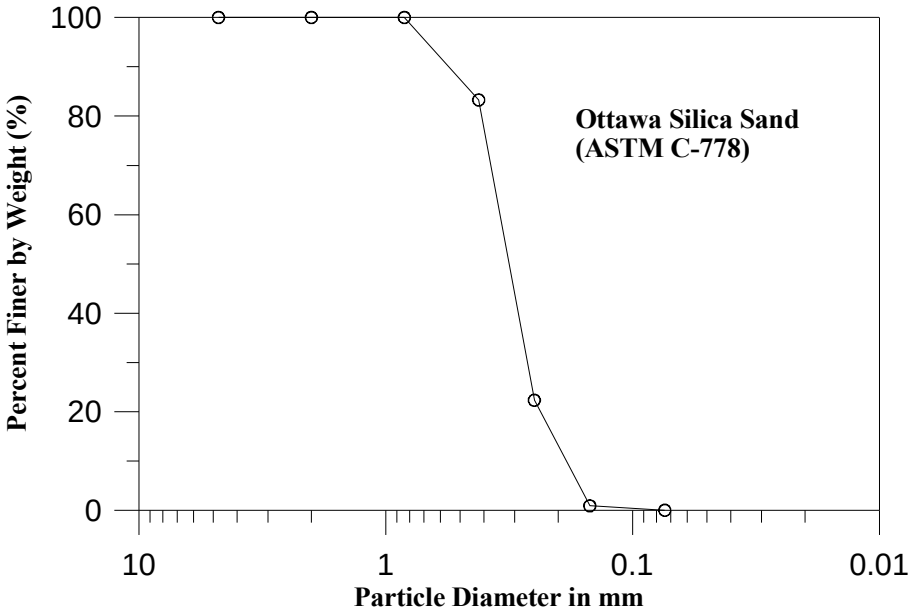

Fig. 9. Grain size distribution of Ottawa sand (after Hou, 2006)

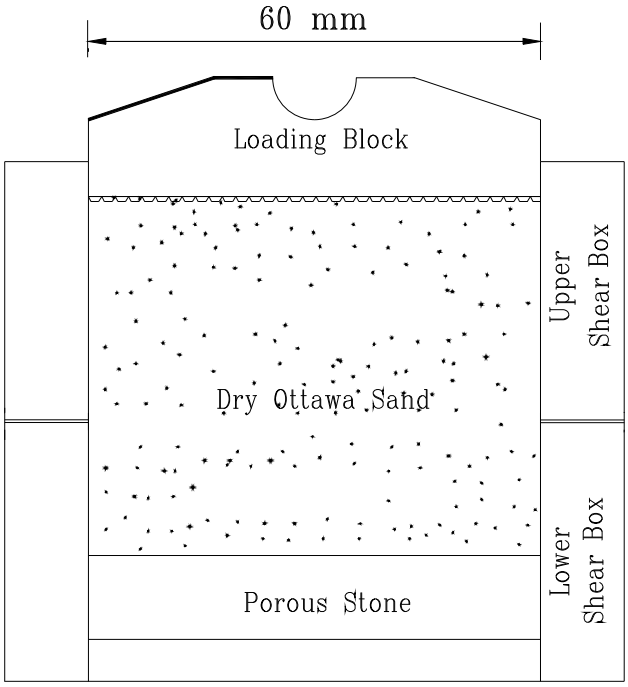

Unit : mm

Fig. 10. Shear Box of Direct Shear Test Device
(after Wu, 1992)

5. TEST RESULTS FOR LOOSE SAND

5.1 Testing Procedure

The testing procedures adopted for this report for the measurement of relative density and stresses in the loose backfill are briefly described below.

For the measurement of the relative density:

(1) Sand pluviated into the soil bin by controlling the drop height of soil and slot opening of the sand hopper.

(2) Density cups placed at the different elevations and locations.

(3) After the soil had been filled up to 1.5 m from the bottom of the soil bin, soil density cups were dug out from the soil mass carefully.

(4) The weight of the cup and soil was measured and recorded.

For the measurement of the earth pressures:

(1) Sand pluviated into the soil bin by controlling the drop height of soil and slot opening of the sand hopper.

(2) Placed the SPTs at the desired locations.

(3) When the backfill was filled up to 1.5 m, the earth pressures were recorded and stored.

5.2 Distribution of Soil Density

To observe the distribution of soil density in the soil bin, the soil density cups were made. The soil density control cup made of acrylic is illustrated in Fig. 11. During the preparation of soil specimen, density cups were buried in the soil mass at different elevations and different locations in the backfill. After the soil had been filled up to 1.5 m from the bottom of the soil bin, soil density cups were dug out from the soil mass carefully. The distribution of soil density with depth for loose sand is shown in Fig. 12. The mean relative density is D_r = 34.1 % with the standard deviation of 2.4%. The soil density distribution was reported by Chen (2002). The test results are in fairly good agreement with data. The backfill achieved with the air-pluviation method was loose, D_r = 15%~50% as suggested by Das (1994).

For comparison purposes, at the beginning of this study, experiments were conducted to investigate the stresses in an uncompacted backfill. Fig. 13 shows the location of soil pressure transducers to measure the distribution vertical earth pressure σ_v with depth. The method to confirm the location and depth of the SPT in the soil mass is shown in Fig. 14. Fig. 15 shows the photograph of SPT used to measure vertical stress in the soil mass. After the backfill had been filled up to 1.5 m thick, the vertical earth pressure σ_v measured in the soil mass was illustrated in Fig. 16. Obviously, the vertical pressure increased with increasing depth and the test data were in good agreement with the equation $\sigma_v = \gamma z$, where γ is the unit weight of the backfill. The locations of soil pressure transducers to measure the distribution of horizontal earth pressure σ_h were shown in Fig. 17. Fig. 18 shows the photograph of SPT used to measure horizontal stress in the soil mass. The distribution of horizontal earth pressure σ_h with depth was illustrated in Fig. 19. In the figure, the earth pressure profile induced by the 1500 mm-thick loose backfill was approximately linear and was in good agreement with the Jaky's equation. Mayne and Kulhawy (1982), Mesri and Hayat (1993) reported the Jaky's equation is suitable for backfill in its loosest

state. From a practical point of view, it may be concluded that for a loose backfill, the vertical and horizontal earth pressure in the soil mass can be properly estimated with the equation $\sigma_v = \gamma z$ and Jaky's equation, respectively.

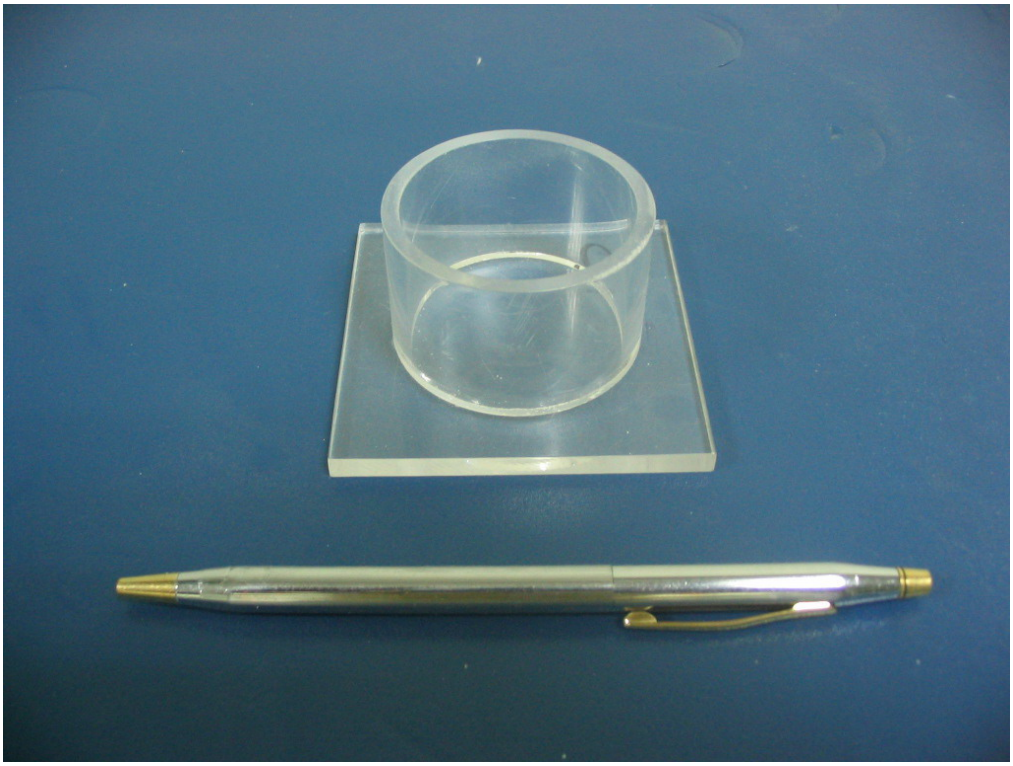

Fig. 11. Soil-density cup

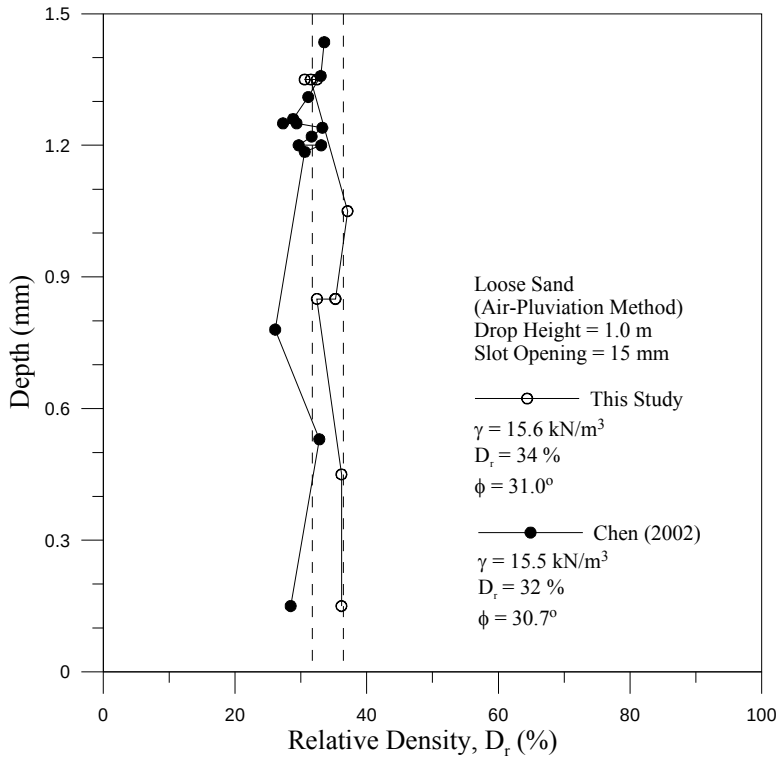

Fig. 12. Distribution of Soil Density for Loose Sand

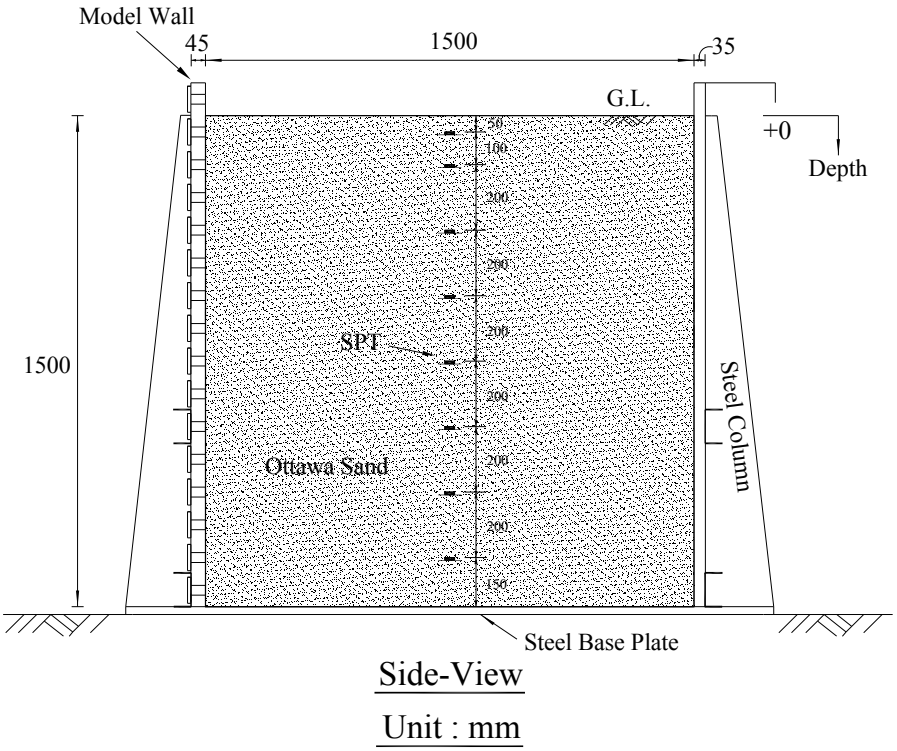

Fig. 13. Locations of SPT to Measure Distribution of Vertical Earth Pressure

Fig. 14. Placement of SPT in Soil Mass

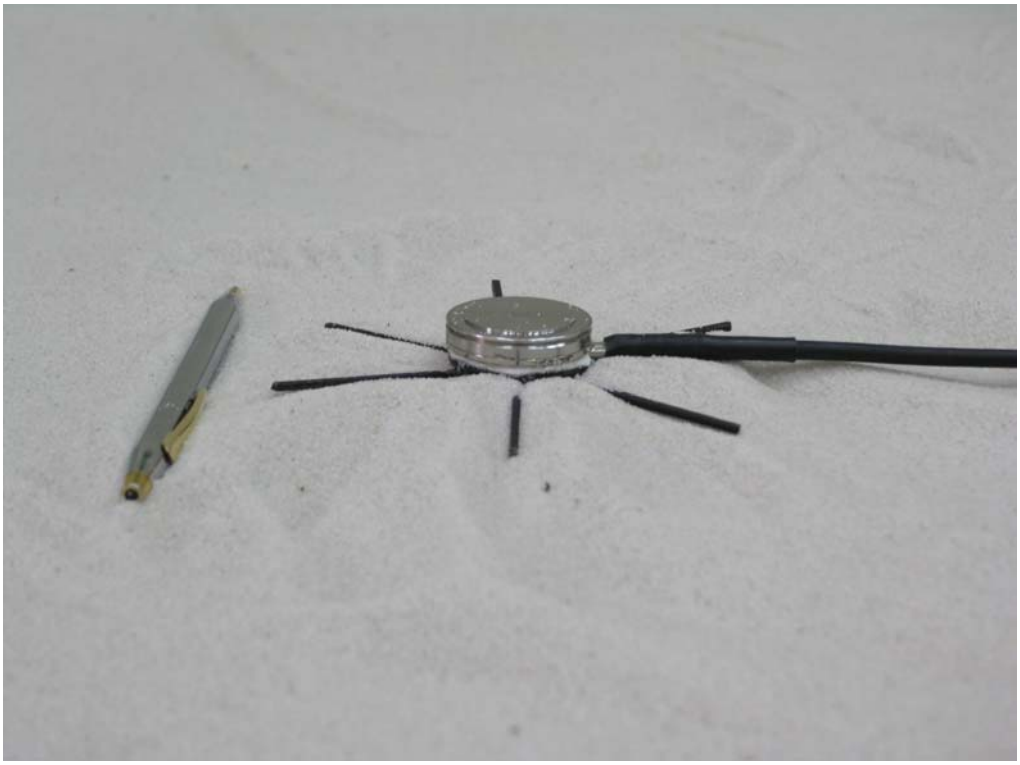

Fig. 15. SPT used to Measured Vertical Stress

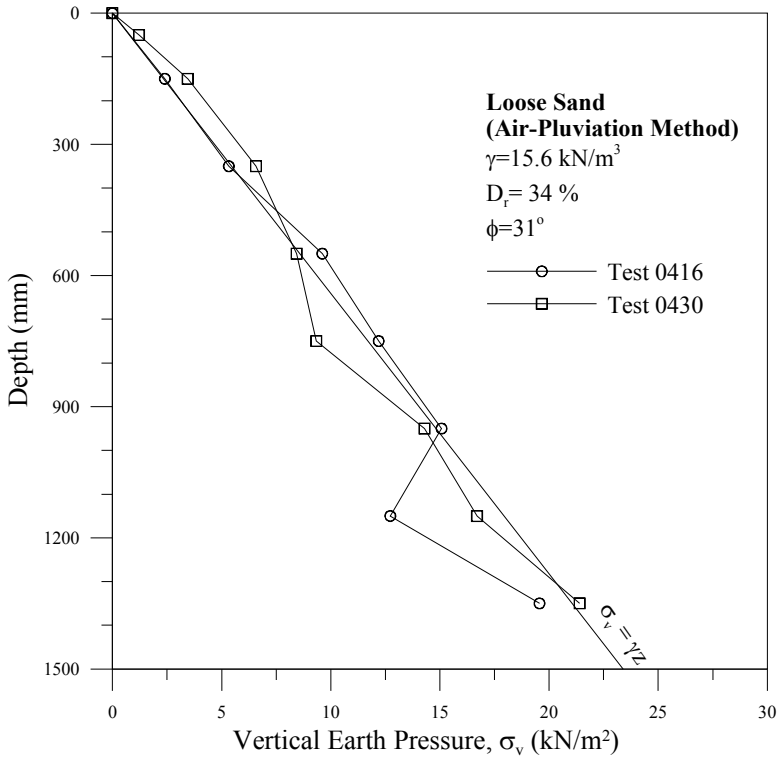

Fig. 16. Distribution of Vertical Earth Pressure

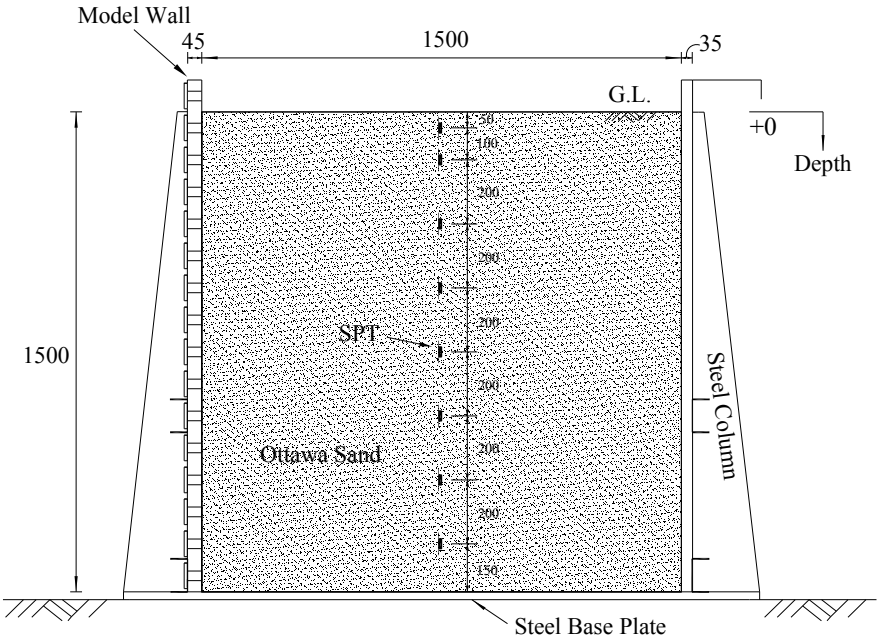

Fig. 17. Locations of SPT to Measure Distribution of Horizontal Earth Pressure

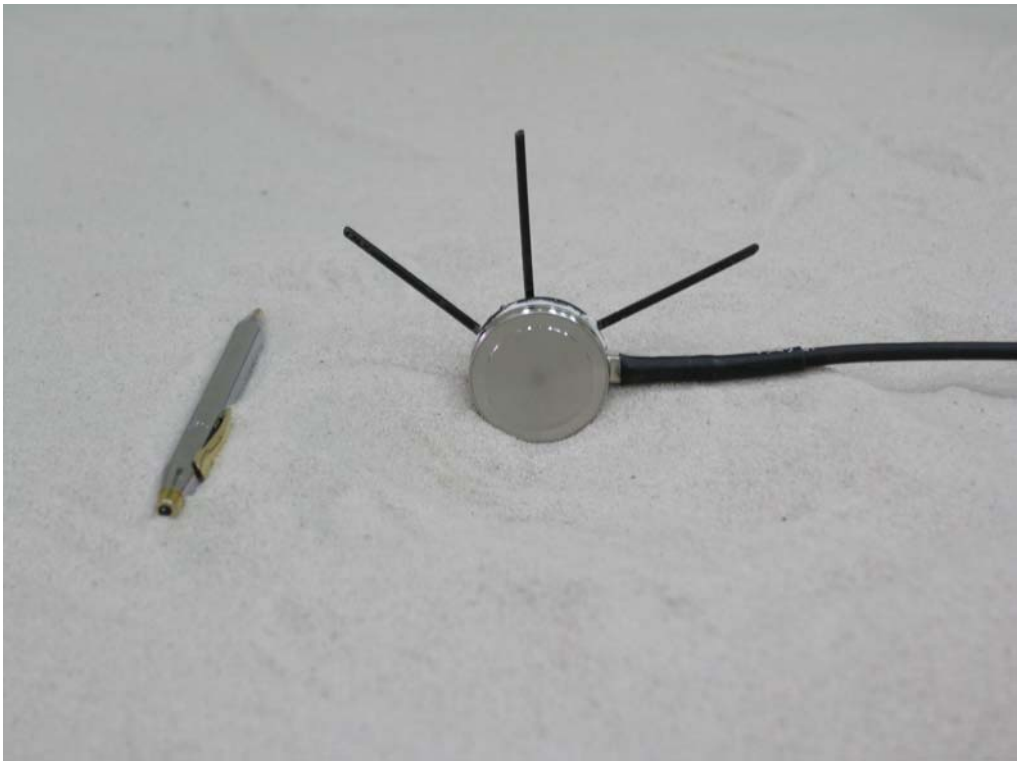

Fig. 18. SPT used to Measured Horizontal Stress

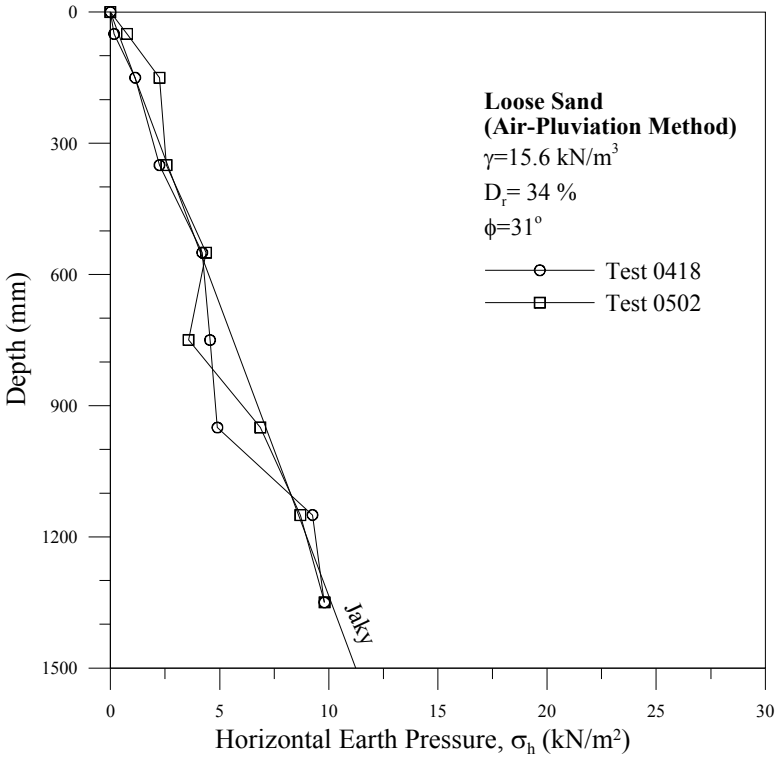

Fig. 19. Distribution of Horizontal Earth Pressure

6. VARIATION OF EARTH PRESSURE DUE TO COMPACTION

6.1 Testing Procedure

The testing procedures adopted for the measurement of the surface settlement and the change of relative density due to compaction is briefly described below.

(1) Sand pluviated into the soil bin by controlling the drop height of soil and slot opening of the sand hopper.
(2) Density cups placed at the different elevations and locations.
(3) After the soil had been filled up to 1.5 m from the bottom of the soil bin, level the surface of the backfill.
(4) After the first pass of the vibratory compactor, remove the compactor.
(5) Measured the surface settlement on the XZ and YZ – plane..
(6) Soil density cups were dug out from the soil mass carefully. Weight of the cup and soil was measured and recorded.
(7) Repeated steps (1) through (6), change the number of passes of the compactor to 2, 4, and 8 passes.

The testing procedures adopted for the measurement of change of the stresses after compaction are briefly described below.

(1) Sand pluviated into the soil bin by controlling the drop height of soil and slot opening of the sand hopper.

(2) SPTs placed in the soil bin at the different elevations and locations.

(3) After the soil had been filled up to 1.5 m from the bottom of the soil bin, level the surface of the backfill.

(4) After the first pass of the compactor, remove the vibratory compactor.

(5) The test data were recorded and stored.

(6) Repeated steps (1) through (5), change the number of passes of the compactor to 2, 4 and 8 passes.

6.2 Surface Settlement and Density Change due to Compaction

The testing procedure of strip compaction was indicated in Fig. 20. The vibratory compactor was pulled over the compaction lane from the left sidewall to the right sidewall for the first pass as shown in Fig. 21. Then the vibratory compactor was turned around 180 degrees to compact the backfill at the second pass from the right to the left sidewall. As the end, the backfill below the compaction lane had been compacted with eight passes of the vibratory compactor. Each pass was about 1.5 m-long and lasted for 70 seconds.

Because of the sidewall friction, the surface settlement measured near the sidewall was less than the average settlement indicated in Fig. 22. Based on the test results, sidewall effects were limited to the regions about 300 mm from the sidewalls.

Before compaction, the height of backfill was 1.5m and the surface of the backfill was horizontal. Fig.23 shows the surface settlement profiles after 1, 2, 4 and 8 passes of the compactor. It is obvious in the figure that the surface settlement increased with the increasing

compaction effort. Fig. 24 shows the surface settlement increased with the increasing number of passes of the compactor. After compactor was pulled horizontally by the operator on the compaction lane, the surface settlement was not uniform.

By controlling the drop height of soil and slot opening of the sand hopper, a loose sand specimen (D_r = 34%) was prepared testing. Fig. 25 shows the contours of relative density in soil mass after the first passage of the compactor. In Fig. 26, Fig. 27, and Fig. 28, the region of dense sand (D_r = 60% ~ 80%) expanded with the increasing number of the compactor passes. The maximum relative density below the compactor was 68%, 72%, and 75%, respectively. The relative density 64%, 68%, 72% and 75% are correspond to the dry unit weight 16.3 kN/m^3, 16.4 kN/m^3, 16.5 kN/m^3 and 16.6 kN/m^3, respectively.

6.3 Change of Vertical Stresses due to Compaction

In Fig. 29, it is seen that the contours of $\Delta\sigma_v$ after the first passage of the compactor were analogous to concentric circles. The center of the concentric circles corresponding to the max $\Delta\sigma_v$ was located at the depth of 300 mm below the compactor. The $\Delta\sigma_v$ would decrease gradually from the central region. Before compaction, vertical stress at the depth of 300 mm calculated by $\sigma_v = \gamma z$ was 4.68 kN/m^2. The incremental vertical stress $\Delta\sigma_v$ was 2.2 kN/m^2 and the incremental stress ratio was 53.0%. In Fig. 28, the relative density of soil changed from the initial value 34% to the maximum value of 72%. At z = 300 mm, the vertical stress increment due to the change of γ (from 15.6 kN/m^3 to 16.6 kN/m^3) was 0.30 kN/m^2. The Comparison between 2.2 kN/m^2 and 0.30 kN/m^2, indicated that the vertical stress increment $\Delta\sigma_v$ was not only affected by change of unit weight of soil. The change of the vertical stress was related to the compaction-induced stresses.

It may be concluded that the compaction-induced vertical stresses were quite significant below the compactor. As the number of passes increased to 2, 4, and 8, more compaction energy was input into the soil mass. In Fig. 30, Fig. 31, and Fig. 32, the contours showed that the depth of the compaction-induced zone increased with increasing energy input. The vertical stress increment $\Delta\sigma_v$ increased with increasing number of passages of the compactor.

6.4 Change of Horizontal Stresses due to Compaction

In Fig. 33, the contours of $\Delta\sigma_h$ formed two circles of stresses at the depth of 300 mm below the edge of the compactor. The $\Delta\sigma_h$ gradually decreased with increasing depth and the distance from the compactor. At z = 300mm, the initial horizontal stress at the depth of 300 mm calculated by Jaky's equation was 2.27 kN/m^2. The incremental horizontal stress $\Delta\sigma_h$ was up to 1.40 kN/m^2 and the stress incremental ratio was 62 %. It may be concluded that the compaction-induced horizontal stresses were quite obvious below the compactor. When the number of passes of the compactor increased to 2 passes, the two circles of high stresses remained below the edge of the compactor as shown in Fig. 34. After 2 – passes of the compactor, $\Delta\sigma_h$ increased to 1.6 kN/m^2. However, as the number of passes of the compactor increased to 4 and 8 passes, the double high stress circles disappeared, and the contours of $\Delta\sigma_h$ were analogous to concentric circles in Fig. 35 and Fig. 36. It is clear that the depth of the compaction-induced zone increased with increasing compaction energy input.

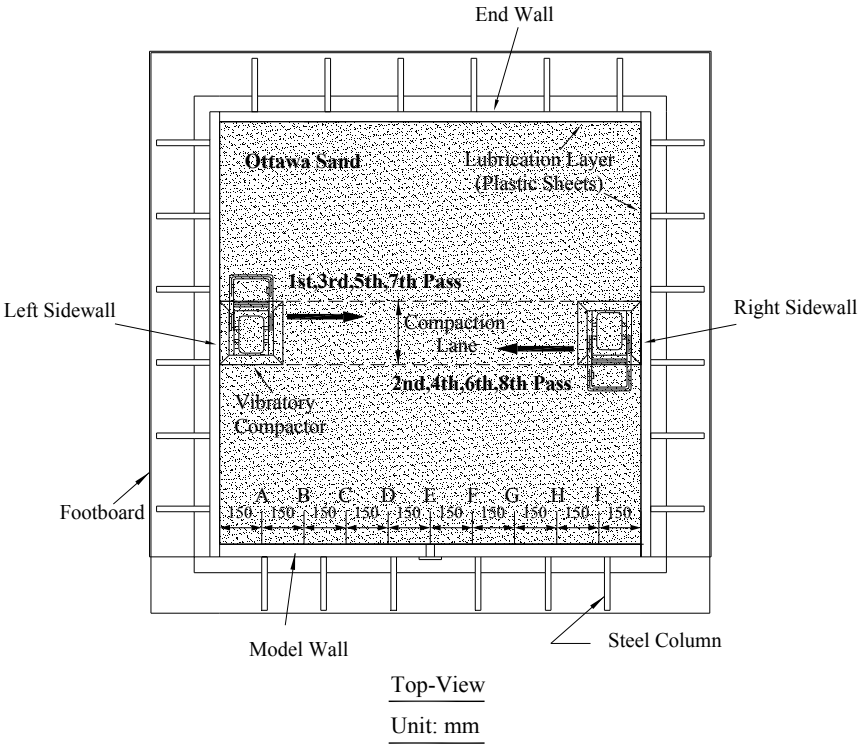

Fig. 20. Testing Procedure of Strip Compaction

Fig. 21. Compaction on Surface of Backfill

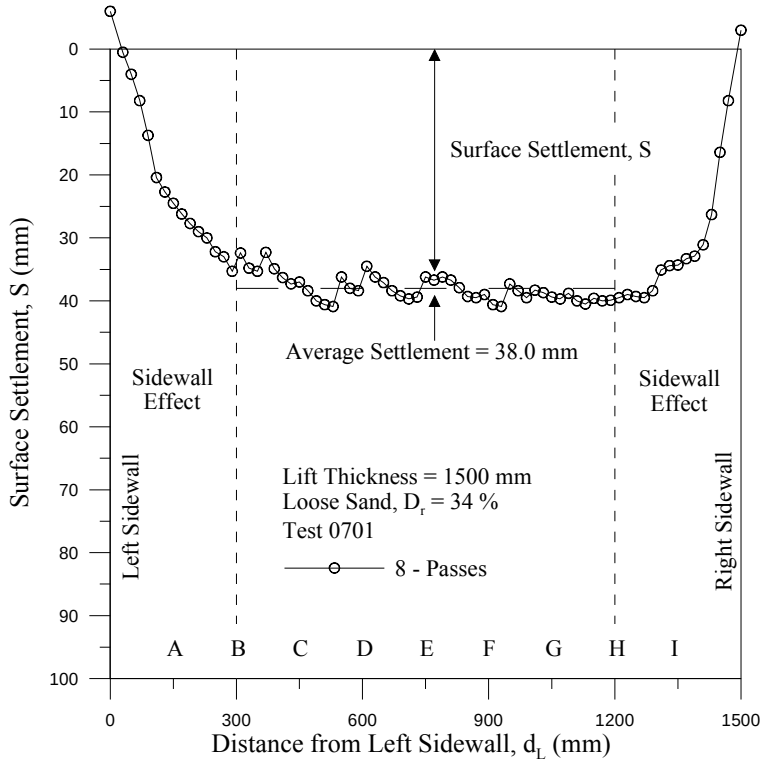

Fig. 22. Surface Settlement along Compaction Lane with Regions of Sidewall Effects

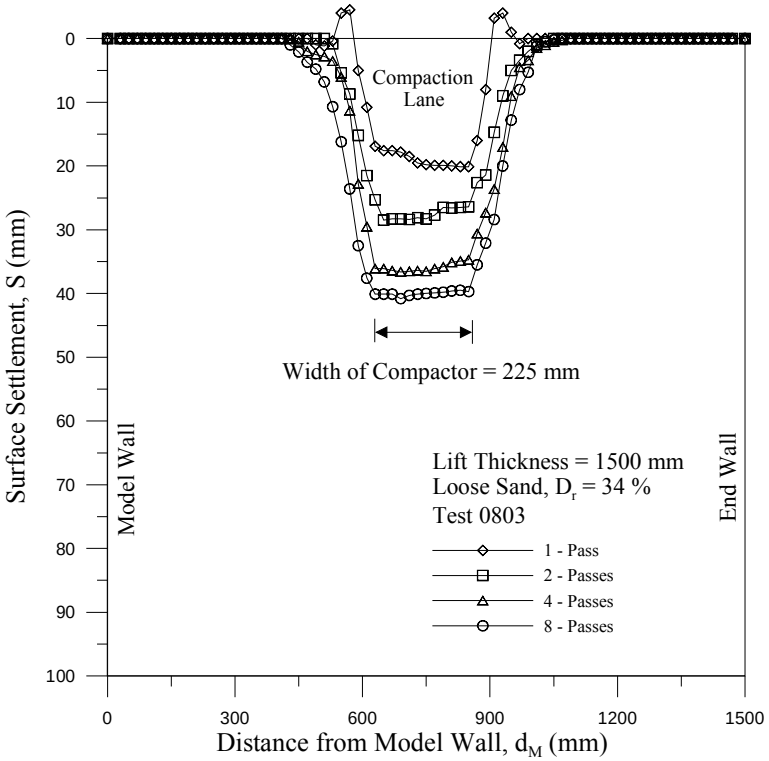

Fig. 23. Surface Settlement of Compaction Lane after 1, 2, 4 and 8 Passes of Compactor

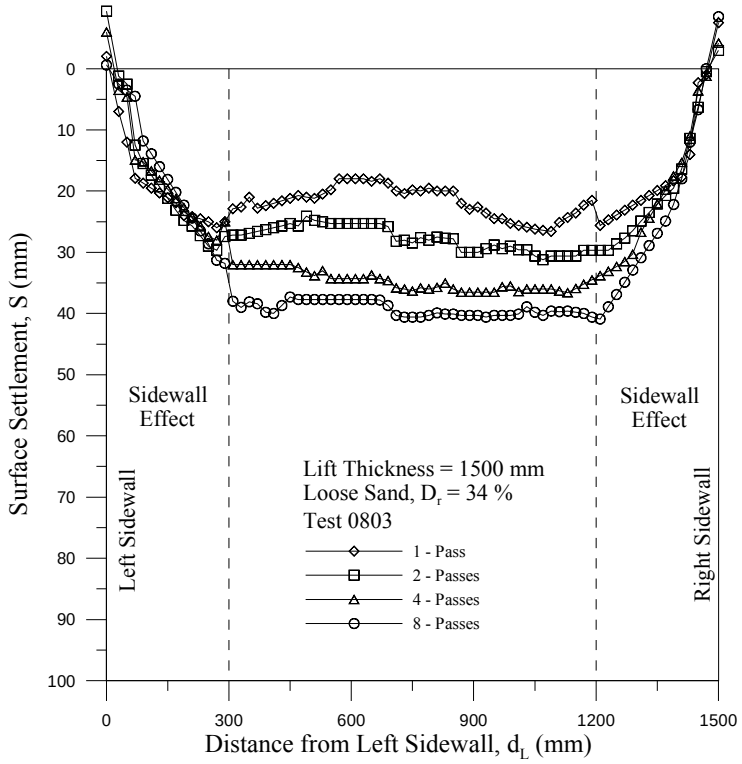

Fig. 24. Surface Settlement along Compaction Lane after 1, 2, 4 and 8 Passes of Compactor

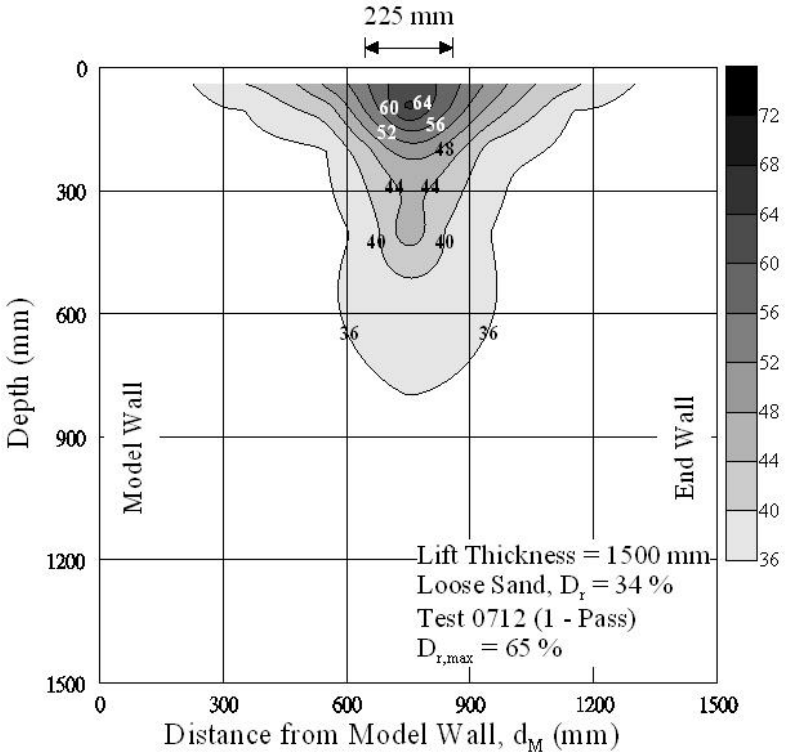

Fig. 25. Contours of Relative Density after 1 – Pass of Compactor

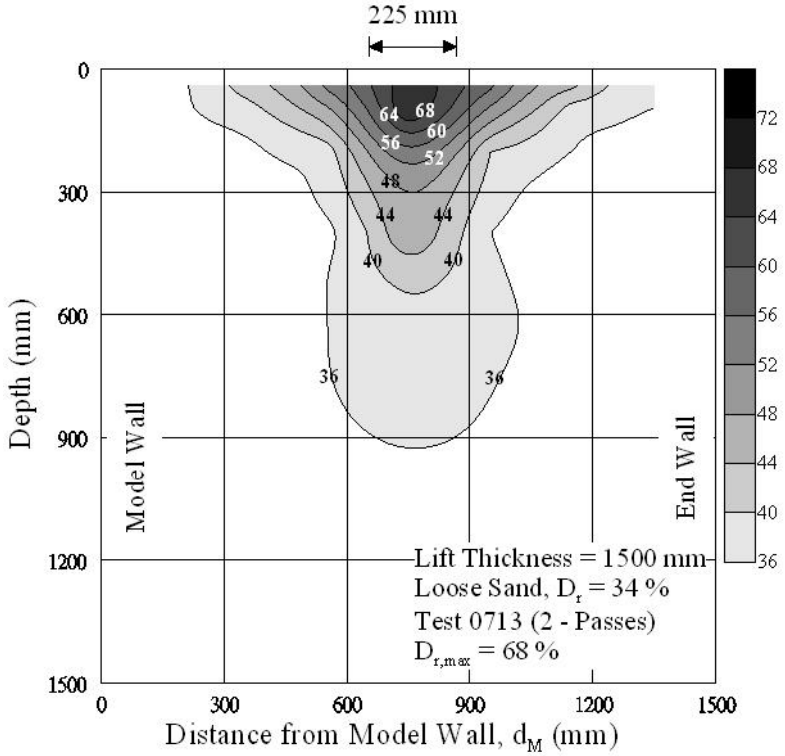

Fig. 26. Contours of Relative Density after 2 – Passes of Compactor

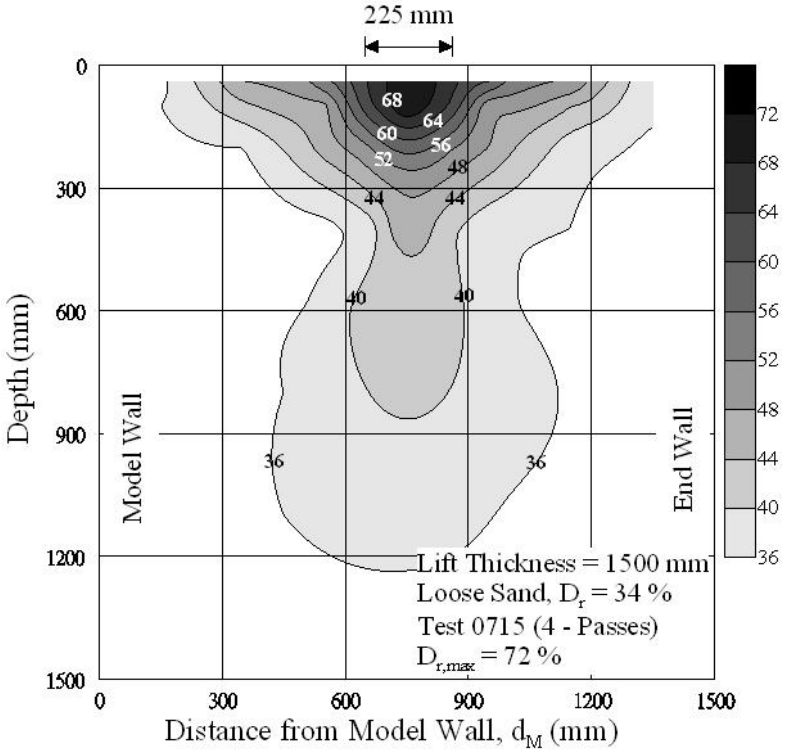

Fig. 27. Contours of Relative Density after 4 – Passes of Compactor

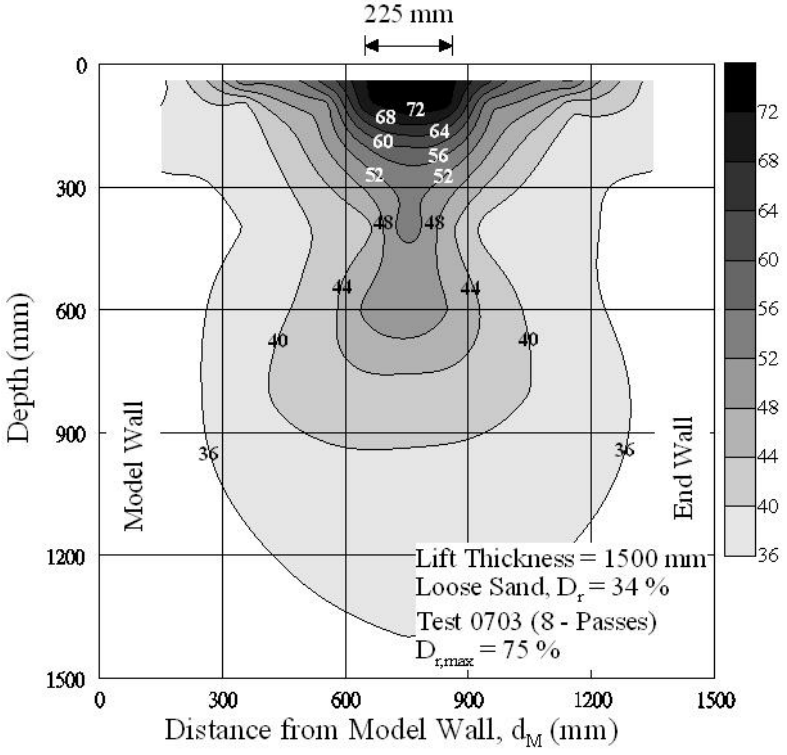

Fig. 28. Contours of Relative Density after 8 – Passes of Compactor

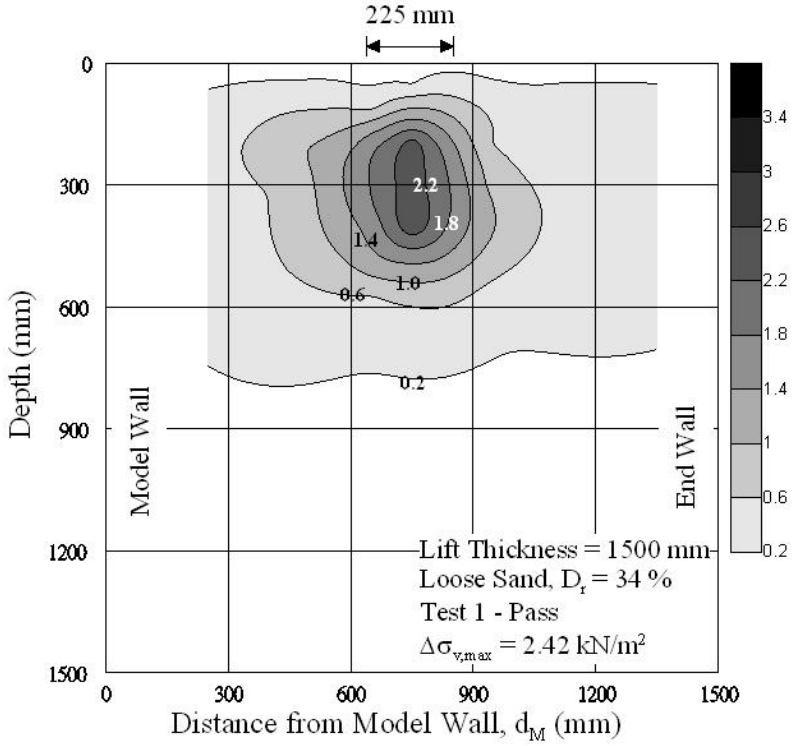

Fig. 29. Contours of $\Delta\sigma_v$ after 1 – Pass of Compactor

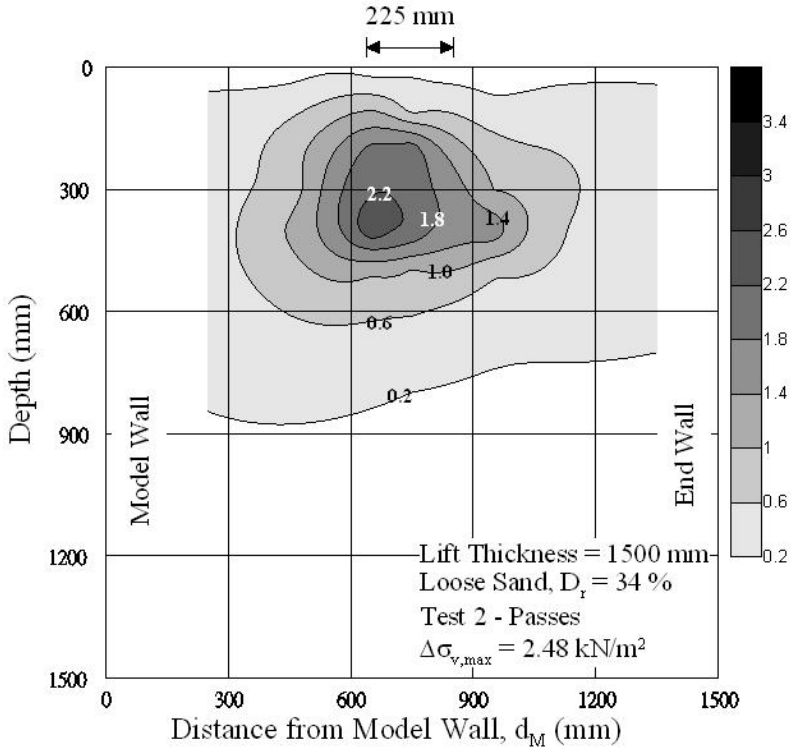

Fig. 30. Contours of $\Delta\sigma_v$ after 2 – Passes of Compactor

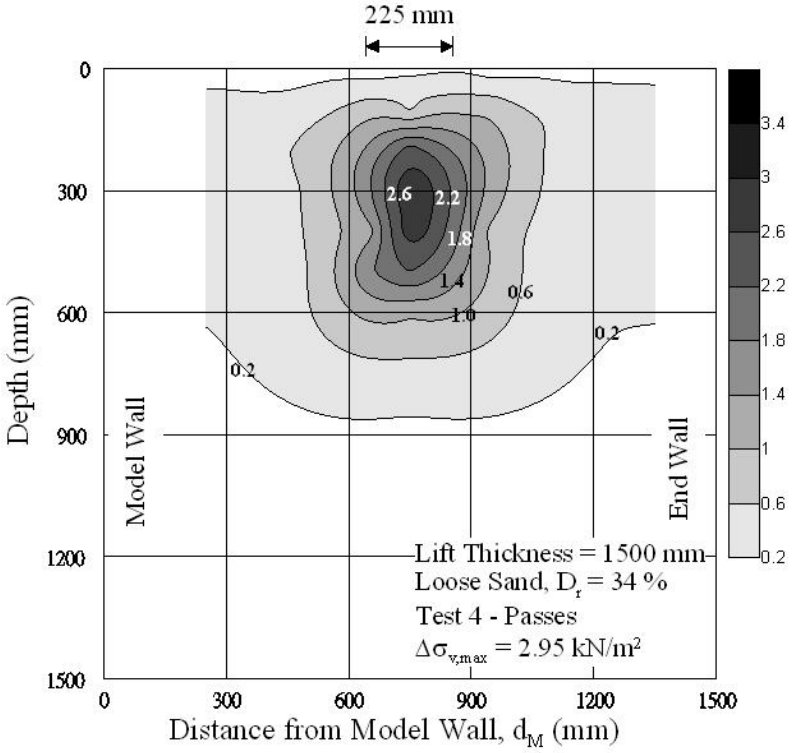

Fig. 31. Contours of $\Delta\sigma_v$ after 4 – Passes of Compactor

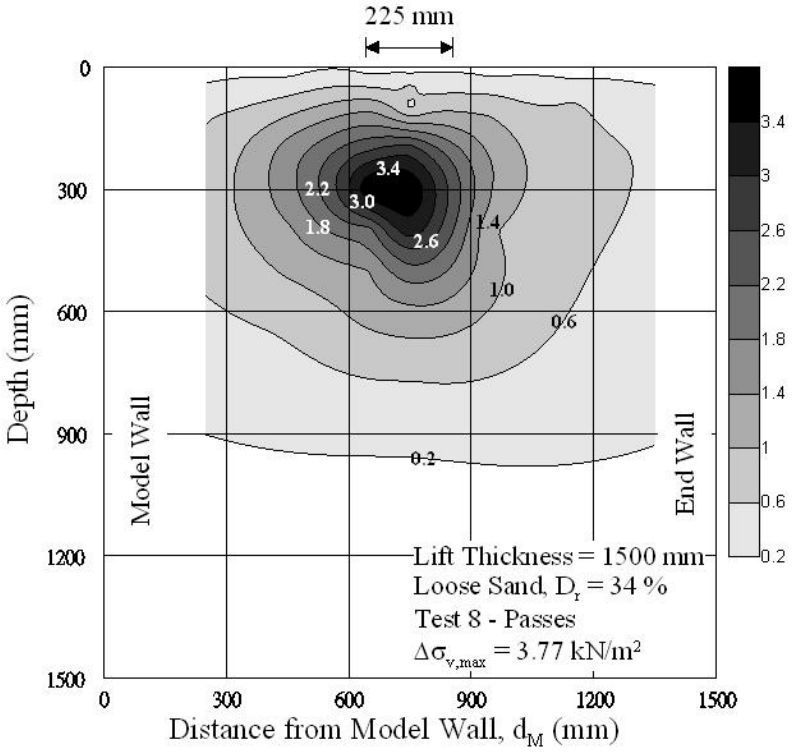

Fig. 32. Contours of $\Delta\sigma_v$ after 8 – Passes of Compactor

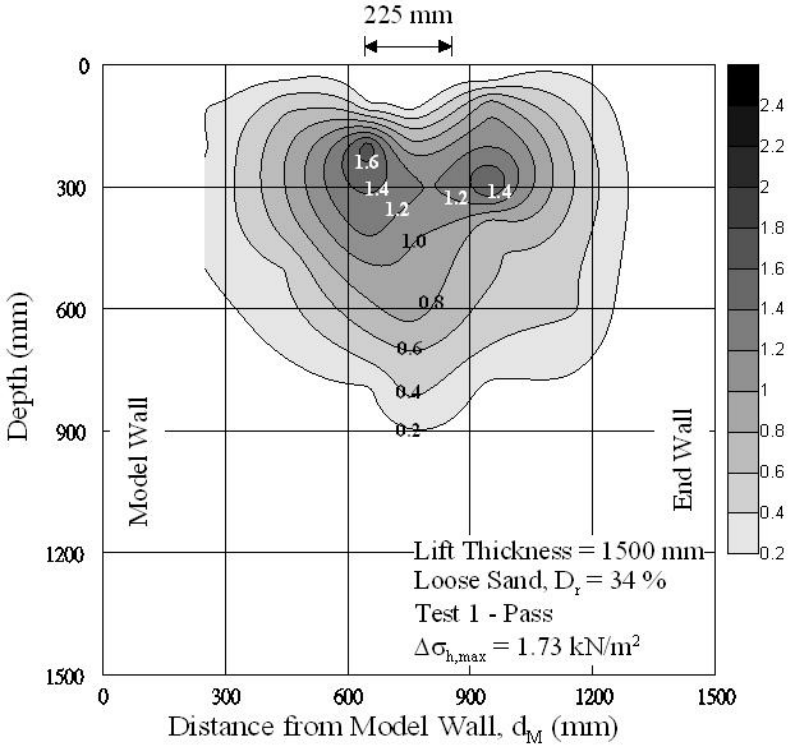

Fig. 33. Contours of $\Delta\sigma_h$ after 1 – Pass of Compactor

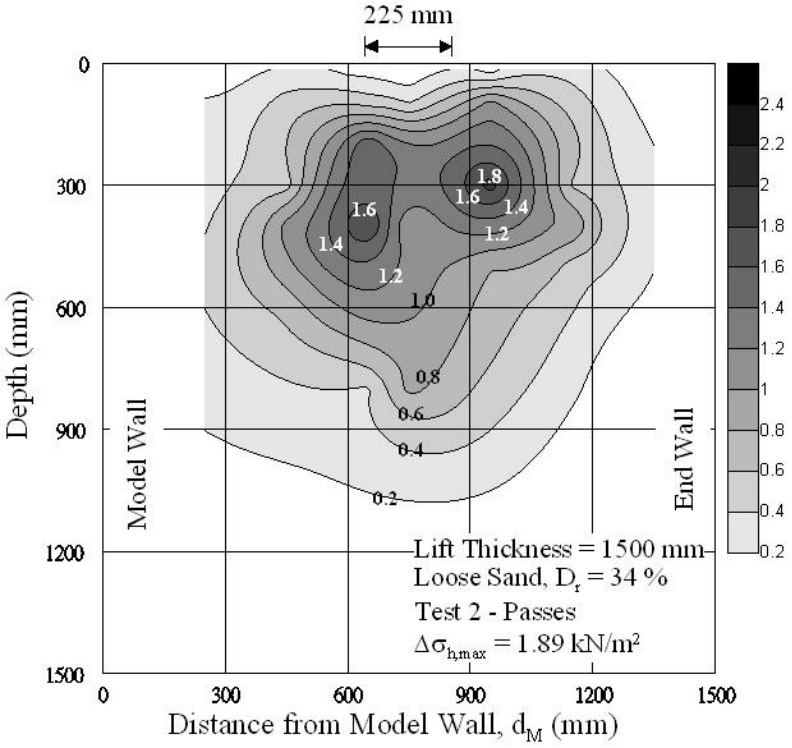

Fig. 34. Contours of $\Delta\sigma_h$ after 2 – Passes of Compactor

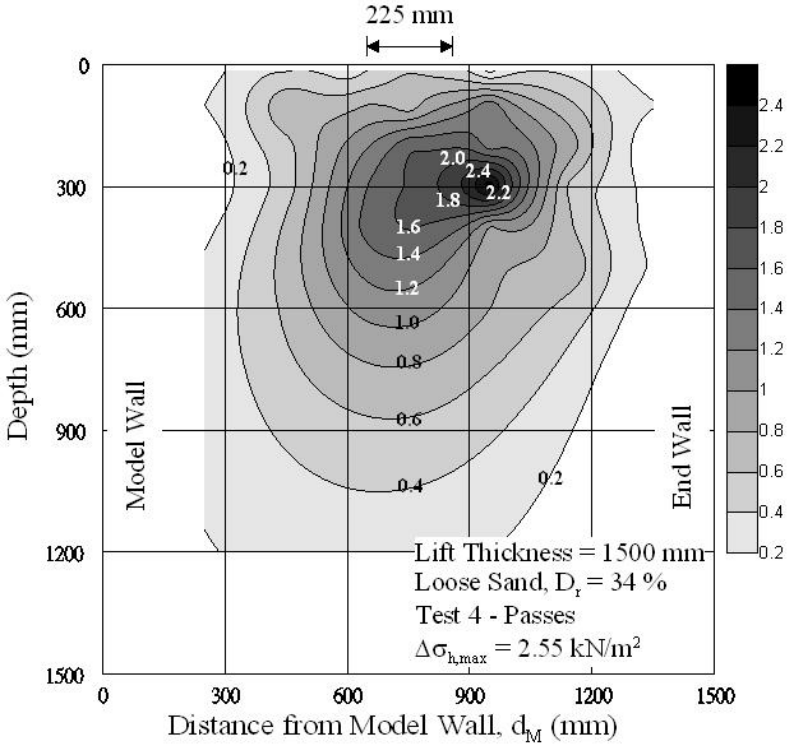

Fig. 35. Contours of $\Delta\sigma_h$ after 4 – Passes of Compactor

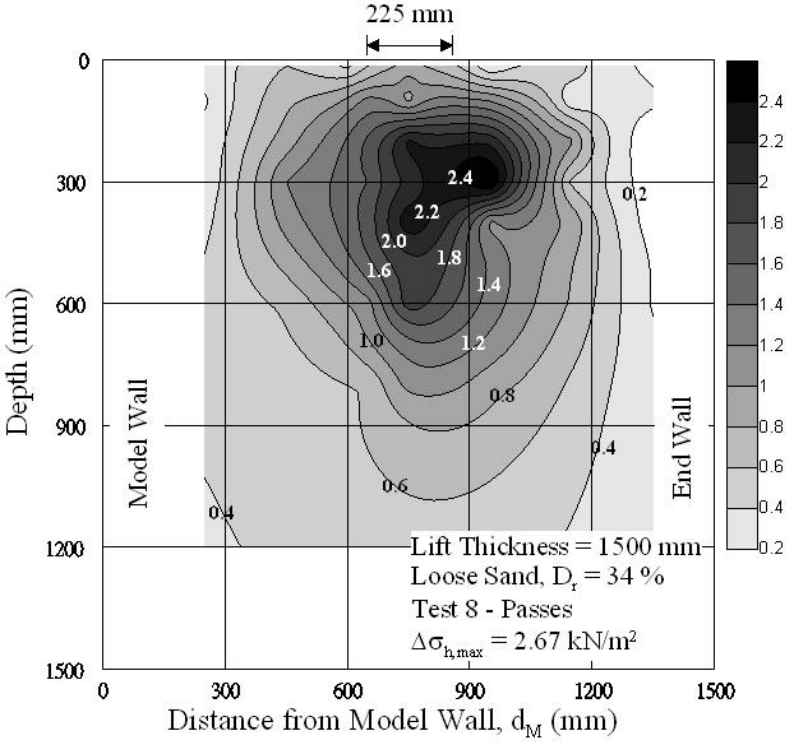

Fig. 36. Contours of $\Delta\sigma_h$ after 8 – Passes of Compactor

7. CONCLUSIONS

In this study, the effects of strip compaction on sand are investigated. Based on the test results, the following conclusions can be drawn.

1. For loose sand, the vertical and horizontal earth pressure in the soil mass could be properly estimated with the equation $\sigma_v = \gamma z$ and Jaky's equation, respectively.
2. The surface settlement increased with the increasing number of passes of the compactor. The relationship between the surface settlement and the number of passes of the compactor could be modeled by the hyperbolic model.
3. After compaction, the range of contours of relative density (D_r = 36 %) would become larger with increasing number of passes.
4. The contours of $\Delta\sigma_v$ were analogous to concentric circles, and the $\Delta\sigma_v$ would decrease gradually from the central region. The vertical stress increment $\Delta\sigma_v$ increased with increasing number of passages of the compactor.
5. The contours of $\Delta\sigma_h$ formed two circles of high stresses and $\Delta\sigma_h$ decreased gradually from the center region after the first and the second passes of compactor. The contours of $\Delta\sigma_h$ were analogous to concentric circles after 4 and 8 passes of the compactor. The depth of the compaction-induced zone increased with increasing compaction energy input.
6. Based on the test results, the mechanism of soils after the first pass of the compactor could be explained by local shear failure. However, the mechanism of soils after 8 passes of the compactor could be simulated by a steel square pile driven in sand with a vibratory hammer.

8. REFERENCES

1. Burgess, G. P. (1999). "Performance of Two Full-scale Model Geosynthetic Reinforced Segmental Retaining Walls," MS thesis, Royal Military College of Canada, Kingston, Ontario, 207.
2. Chang, S. Y. (2000). "Effects of Backfill Density on Active Earth Pressure." MS thesis, Dept. of Civil Engineering, National Chiao Tung University, Hsinchu, Taiwan.
3. Chen, T. J. (2002). "Earth Pressure due to Vibratory Compaction." Ph.D. Dissertation, Department of Civil Engineering, National Chiao Tung University, Hsinchu, Taiwan.
4. Chen, T. J., and Fang, Y. S, (2002). "A New Facility for Measurement of Earth Pressure At-Rest," *Geotechnical Engineering Journal*, SEAGS, 3(12), 153-159.
5. Chen, T. J., (2003). "Earth Pressure Due to Vibratory Compaction", Doctor of Philosophy Dissertation, National Chiao Tung University, Hsinchu, Taiwan.
6. D'Appolonia, D. J., Whitman, R. V., and D'Appolonia, E. (1969). "Sand Compaction with Vibratory Rollers." *Journal of the Soil Mechanics and Foundations Division*, ASCE, 95(SM1), 263-284.
7. Das, B. M., (1994), "Principal of Geotechnical Engineering. " 3rd Edition, PWS Publishing Company, Boston.
8. Fang, Y. S., Chen, T. J., Holtz, R. D., and Lee, W. F., (2004). "Reduction of Boundary Friction in Model Tests", *Geotechnical Testing Journal*, ASTM, 27(1), 1-10.
9. Filz, G. M., and Duncan J. M. "Earth Pressures due to Compaction: Comparison of Theory with Laboratory and Field Behavior." *Transportation research record*, 1526, 28-37.
10. Ho, Y. C., (1999). "Effects of Backfill Compaction on Passive Earth Pressure." MS thesis, Dept. of Civil Engineering, National Chiao Tung University, Hsinchu, Taiwan.
11. Hou, P. H. (2006). "Design and Construction of NCTU K_A Model Retaining Wall." MS

thesis, Dept. of Civil Engineering, National Chiao Tung University, Hsinchu, Taiwan.
12. Huang, C. C., Cheng, C. Y., Hsia, S. H., and Hsu, S. P. (1994). "Reinforcement Stiffness on Load-deformation Characteristics of Reinforcement." *Proceedings of the Fifth International Conference on Geotextiles, Geomembranes, and Related Products*, Singapore, 1, 197-200.
13. Kumbhojkar, A. S. (1993) "Numerical Evaluation of Terzaghi's N_γ." *Journal of Geotechnical Engineering,* American Society of Civil Engineers, 119(3), 598-607.
14. Lo Presti, D. C. F., Pedroni, S., and Crippa, V. (1992). "Maximum Dry Density of Cohesionless Soils by Pluviation and by ASTM D 4253-83: A comparative study." *Geotechnical Testing Journal*, ASTM, 15(2), 180-189.
15. McElroy, J. A. (1997). "Seismic Stability of Geosynthetic Reinforced Slopes: A shaking table study." MS thesis, University of Washington, Seattle, 286.
16. Mesri, G., and Hayat, T. M. (1993). "The Coefficient of Earth Pressure at rest." *Canadian Geotechnical Journal*, 30(4), 647-666.
17. Rad, N. S., and Tumay, M. T. (1987). "Factors affecting sand specimen preparation by raining." *ASTM Geotechnical Testing Journal*, 10(1), 31-37.
18. Seed, R. B., and Duncan, J. M. (1983). "Soil-Structure Interaction Effects of Compaction-induced Stresses and Deflections." *Geotechnical Engineering Research Report No. UcB/GT/83-06*, Univ. of California Berkeley, CA.
19. Tzeng, S. K., (2002). "Horizontal Pressure on an Unyielding Wall due to Strip Loading on Backfill with Different Densities." MS thesis, Dept. of Civil Engineering, National Chiao Tung University, Hsinchu, Taiwan.
20. Wu, F. J., (1992). "Effects of Adjacent Rock Face Inclination on Earth Pressure at-rest." MS thesis, Dept. of Civil Engineering, National Chiao Tung University, Hsinchu, Taiwan.
21. Wu, B. F., (1992). "Design and Construction of National Chiao Tung University Model Retaining Wall." MS thesis, Dept. of Civil Engineering, National Chiao Tung University, Hsinchu, Taiwan.
22. Yang, J. (2006). "Influence Zone for End Bearing of Piles in Sand." *Journal of Geotechnical Geoenvironmental Engineering*, ASCE, 132(9), 1229-1237.

9. 計劃成果自評：

本研究探討條形振動夯實造成砂土密度和土壓力的變化。本研究以氣乾之渥太華砂為回填土，回填土高 1.5 公尺。回填土初始相對密度為 34%。為了在實驗室模擬雙向平面應變的情況，本研究採用塑膠膜潤滑層來降低砂土和填砂槽側牆間的摩擦力。根據實驗結果，本研究獲得以下幾項結論：

1. 對於疏鬆砂土，土體內的垂直土壓力和水平土壓力可分別以 $\sigma_v = \gamma z$ 和 Jaky 公式來進行合理的估算。
2. 隨著夯實機夯實趟數的增加，條形夯實區之地表沉陷量隨之增大。地表沉陷量和夯實趟數之間的關係可以用雙曲線的模式來模擬。
3. 砂土的相對密度變化等高線範圍，會隨著夯實趟數增加而擴大。
4. 垂直土壓力變化量的等高線近似於同心圓的形狀，而殘餘垂直土壓力 $\Delta\sigma_v$ 會由圓心區域向外逐漸減少。土體內最大 $\Delta\sigma_v$ 值會隨著夯實趟數增加而增大。
5. 在夯實機夯實 1 和 2 趟後，殘餘水平土壓力 $\Delta\sigma_h$ 的等高線會形成兩個較高的應力區，水平土壓力變化量會由中心區域逐漸減少。然而在夯實機夯實 4 和 8 趟後，殘餘水平土壓力的等高線則近似於一個同心圓的形狀。夯實影響的區域 ($\Delta\sigma_h = 0.2$ kN/m^2 應力等高線) 深度會隨著夯實能量增加而增大。
6. 在夯實一趟後，土壤所受夯實影響的機制可以用基礎下方土壤之局部剪力破壞的情況來解釋。然而，當夯實趟數增加到 8 趟後，被夯實土壤之機制可用方形鋼樁以振動打樁機貫入砂質地盤的情況來模擬。本研究內容與計劃書完全相符。

本研究獲得數項創新發現，具工程實用價值，上述該研究成果已於2009年10月於埃及亞歷山卓市(Alexandria, Egypt)舉行的第17屆國際土壤力學及大地工程研討會(17th International Conference on Soil Mechanics and Geotechnical Engineering)發表，獲得國際大地工程界肯定，充分達成計劃目標。參與研究的碩士班研究生籍此機會，習得大型基礎模型實驗與資料擷取之操作，以及嚴謹審慎之實驗方法與獨立思考及創造的能力，獲益匪淺。

可供推廣之研發成果資料表

□ 可申請專利　□ 可技術移轉　日期：99 年 08 月 10 日

國科會補助計畫	計畫名稱：震動夯實造成之土壤應力及密度變化（Ⅱ） 計畫主持人：方永壽 教授 計畫編號：NSC 98-2221-E-009-135- 學門領域：土木水利工程
技術/創作名稱	震動夯實造成之土壤應力及密度變化
發明人/創作人	方永壽 教授
技術說明	中文: 本研究利用國立交通大學模型擋土牆設備探討震動夯實所引致之土體密度及應力變化。以氣乾渥太華砂作為回填土進行夯實，回填土高 1.5 公尺。回填土初始相對密度為 34%時地表震動夯實對砂土密度與土壓力之影響。依實驗結果可獲得以下結論。(1) 對於疏鬆砂土，土體內的垂直土壓力和水平土壓力可分別以 $\sigma_v = \gamma z$ 和 Jaky 公式來進行合理的估算。(2) 隨著夯實機夯實趟數的增加，條形夯實區之地表沉陷量隨之增大。地表沉陷量和夯實趟數之間的關係可以用雙曲線的模式來模擬。(3) 砂土的相對密度變化等高線範圍，會隨著夯實趟數增加而擴大。(4) 垂直土壓力變化量的等高線近似於同心圓的形狀，而殘餘垂直土壓力 $\Delta\sigma_v$ 會由圓心區域向外逐漸減少。土體內最大 $\Delta\sigma_v$ 值會隨著夯實趟數增加而增大。(5) 在夯實機夯實 1 和 2 趟後，殘餘水平土壓力 $\Delta\sigma_h$ 的等高線會形成兩個較高的應力區，水平土壓力變化量會由中心區域逐漸減少。然而在夯實機夯實 4 和 8 趟後，殘餘水平土壓力的等高線則近似於一個同心圓的形狀。夯實影響的區域深度會隨著夯實能量增加而增大。(6) 在夯實一趟後，土壤所受夯實影響的機制可以用基礎下方土壤之局部剪力破壞的情況來解釋。當夯實趟數增加到 8 趟後，被夯實土壤之機制可用方形鋼樁以振動打樁機貫入砂質地盤的情況來模擬。

	英文： This report studies the variation of soil density and earth pressure due to the strip compaction with a vibratory compactor. In this study, dry Ottawa sand was used as backfill material, and the height of backfill was 1.5 m. The initial relative density of the backfill was 34 %. To simulate a 2-way plane strain condition in the laboratory, the friction between the soil and sidewalls of the soil bin was reduced as much as possible. Based on the test results, the following conclusions can be drawn. 1. For loose sand, the vertical and horizontal earth pressure in the soil mass could be properly estimated with the equation $\sigma_v = \gamma z$ and Jaky's equation, respectively. 2. The surface settlement increased with the increasing number of passes of the compactor. The relationship between the surface settlement and the number of passes of the compactor could be modeled by the hyperbolic model. 3. After compaction, the range of contours of relative density (D_r = 36 %) would become larger with increasing number of passes. 4. The contours of $\Delta\sigma_v$ were analogous to concentric circles, and the $\Delta\sigma_v$ would decrease gradually from the central region. The vertical stress increment $\Delta\sigma_v$ increased with increasing number of passages of the compactor. 5. The contours of $\Delta\sigma_h$ formed two circles of high stresses and $\Delta\sigma_h$ decreased gradually from the center region after the first and the second passes of compactor. The contours of $\Delta\sigma_h$ were analogous to concentric circles after 4 and 8 passes of the compactor. The depth of the compaction-induced zone increased with increasing compaction energy input. 6. Based on the test results, the mechanism of soils after the first pass of the compactor could be explained by local shear failure. However, the mechanism of soils after 8 passes of the compactor could be simulated by a steel square pile driven in sand with a vibratory hammer.
推廣及運用的價值	本研究屬於基礎學術性研究，一年計劃完成，所獲研究成果將有助於國內外基礎工程設計規劃之參考。

※ 1.每項研發成果請填寫一式二份，一份隨成果報告送繳本會，一份送　貴單位研發成果推廣單位（如技術移轉中心）。

※ **2.本項研發成果若尚未申請專利，請勿揭露可申請專利之主要內容。**

※ 3.本表若不敷使用，請自行影印使用。

行政院國家科學委員會補助參與國際學術會議報告

專題研究計畫補助編號：NSC 98-2221-E-009-135 及 NSC 97-2221-E-009-124

報告人: 方永壽教授
服務機構: 國立交通大學土木工程系所
職稱: 教授

會議名稱: 第 17 屆國際土壤力學及大地工程研討會 (17th International Conference on Soil Mechanics and Geotechnical Engineering)

舉辦地點: Alexandria, Egypt
舉辦時間: 2009 年 10 月 5 日~9 日

主辦單位:

1. International Society of Soil Mechanics and Geotechnical Engineering (ISSMGE)
2. Egyptian Geotechnical Society
3. Government of Egypt
4. City of Alexandria

國科會專題研究計畫補助編號：
NSC 98-2221-E-009-135 及 NSC 97-2221-E-009-124

攜回資料: 研討會論文集 4 大冊及論文集光碟 1 片

一、參加會議經過

國際土壤力學及大地工程研討會 (International Conference on Soil Mechanics and Geotechnical Engineering)是全世界最大、也是最重要的大地工程研討會。這項研討會是由國際土壤力學及基礎工程學會(International Society of Soil Mechanics and Geotechnical Engineering)；埃及大地工程學會(Egyptian Geotechnical Society)；埃及政府(Government of Egypt)；及亞歷山卓市政府(City of Alexandria)共同主辦。本次國際會議有來自 80 餘國家大約 1,200 位代表參與，4 大本論文集共收錄 700 多篇論文。上圖左起為中華民國大地工程學會理事長台科大廖洪鈞教授、計畫主持人方永壽、及中興顧問公司江政恩主任合影於研討會場。

大會於研討會前兩天(2009/10/5 及 2009/10/6)邀請數位知名的大地工程學者發表演講,例如大會於 2009 年 10 月 5 日上午邀請澳洲 Prof. Poulos 進行 Terzaghi Oration 專題演講，介紹中東超高層建築物深基礎面臨的挑戰，大師級學者的報告內容精采，與會者收穫甚為豐富。大會於 2009 年 10 月 5 日下午邀請美國 Georgia Tech.的 Prof. Paul Mayne 進行 State of the Art (SOA #1)專題演講，介紹大地材料行為及試驗(Geomaterial behavior and testing)，報告內容精采，甚具啟發性。下圖左起為交大黃安斌教授、Prof. Paul Mayne、及計畫主持人方永壽於(SOA #1)專題演講後共進午餐時所攝的照片。

本次研討會於研討會後兩天(2009/10/7 及 2009/10/8)，透過下列主題集中的 16 個討論會場次(Parallel Sessions)，由 General Reporter, Panelists 及 Selected Authors 發表經詳細審查、具重要性的論文，進行國際水準的論文發表，促進學術界與工業界的跨領域交流。

1A - Laboratory Testing
1B - Physical and Constitutive Modeling
1C - Problematic Soils and Geosynthetic Material
1D - In-situ Testing
2A - Deep Foundations & Retaining Walls
2B - Slopes and Embankments
2C - Underground Structures
3A - Instrumentation in Geotechnical Engineering
3B - Monitoring and Performance
3C - Interactive Design
4A - Ground Improvement, Grouting and Dredging
4B - Deep Excavation, Tunneling and Groundwater Control
4C - Natural Hazard Mitigation
5A - Owner, Engineer and Contractor Public Awareness
5B - Management of Geotechnical Data and Processes
5C - Training of Geotechnical Engineers/Future of Geotechnical Engineering Education

二、論文刊出

報告人及研究生簡煜倫合著之論文"Variation of soil density and earth pressure due to strip compaction"，被編列在研討會主題 1B (Physical and Constitutive Modeling)，論文被發表在研討會論文集第一冊、第 700 至 704 頁。此項研究依據實驗方法探討條型夯實振動造成砂土密度及土壓力之變化，為國科會專題研究計畫 NSC 95-2211-E-009-199 之研究成果。

三、考察參觀心得

同行參與此項研討會的國內學者包含交通大學黃安斌教授、台灣大學翁作新教授、陳正興教授、林美聆教授、台科大廖洪鈞教授、李維峰博士、中原大學馮道偉教授、淡江大學張德文教授及中興顧問公司江政恩主任等。

3-1 各國代表參加人數

大會公佈至 2009 年 9 月 30 日為止，已註冊報名參加研討會的各國代表名單(List of participants)，總共有來自 81 個國家、大約 1,200 位代表與會，其中代表人數列前 20 名的國家名稱及代表人數如下表所列：

名次	國家名稱(參加人數)	名次	國家名稱(參加人數)
1	Japan (101)	11	Netherlands (27)
2	United States (55)	12	Korea (24)
3	Egypt (53)	13	Canada (21)
4	China (47)	14	Spain (17)
5	France (38)	15	United Kingdom (16)
6	Germany (36)	16	India (16)
7	Australia (35)	17	Greece (15)
8	Italy (34)	18	Taiwan (12)
9	Brazil (31)	19	Hong Kong (12)
10	Russia (27)	20	Turkey (12)

日本是上一屆 16th ICSMGE 的主辦國，埃及是本屆 17th ICSMGE 的主辦國，所以日本與埃及代表人數特別龐大。美國、法國、德國、澳洲及義大利是傳統工程強國，大地工程人才濟濟，所以與會代表特別多。我國註冊出席代表 12 人，大致與我國人口成合理比例。上表中排名第 4 的 China，近年經濟及工程發展有長足的進步，由其代表團人數可以看出其逐步跨入國際舞台之趨勢。

3-2 音樂裊繞的開幕典禮

開幕典禮乃是研討會枯燥乏味又必要的儀式，在 2009 年 10 月 5 日上午的開幕典禮中，埃及政府長官、亞歷山卓市政府長官、國際大地工程學會會長 Prof. Pinto、及 17th ICSMGE 研討會主辦人 Prof. Hamza 依序上台官式致詞。

在長官致詞告一段落後，舞台布幕緩緩升起，舞台上出現一個大約 20 人的弦樂團，如下圖所示。隨著飛舞的指揮棒，他們流暢的奏出具埃及風味的美妙音樂，各國代表心中頓時感覺輕鬆愉快，暫時忘卻無聊的官

式致詞，放下國界與文化藩籬，融入一片愉悅的旋律，這份別出心裁的安排，受到與會者一致的好評。

Variation of soil density and earth pressure due to strip compaction

Variation de la densité et de la poussée du sol due à un compactage en bande

Y.S. Fang
Department of Civil Engineering, National Chiao Tung University, Hsinchu, Taiwan
Y.L. Chien
Power Projects, Civil Dept., E & C Corporation, Taipei, Taiwan

ABSTRACT

This paper studies the variation of soil density and earth pressure in a soil mass due to the vibratory compaction along a strip on the surface of the cohesionless backfill. Experiments were conducted in a non-yielding model retaining wall facility and dry Ottawa sand was used as fill material. Based on the test results, it is found that surface settlement increased with the increasing number of passage of the compactor. The relationship between the surface settlement and the number of passes could be properly described by the hyperbolic model. The contours of $\Delta\sigma_v$ after the first passage of the compactor were analogous to a series of concentric circles. As the number of passes increased to 8, the depth of the compaction-induced zone increased with increasing energy input. After the first passage of the compactor, the contours of $\Delta\sigma_h$ formed two regions of stress concentration below the surface. As the number of passage increased to 8, the two high-stress regions merged. The mechanism of soils after the first passage of the compactor could be properly explained by local-shear bearing capacity failure mode. The mechanism of soils after 8 passes of the compactor could be simulated by a single pile driven into a cohesionless soil.

RÉSUMÉ

Cet article étudie les variations de la densité et de la poussée du sol après le compactage par vibration d'une bande à la surface d'un remblai meuble. Des expériences furent réalisées pour étudier les effets d'un vibro-compacteur sur la densification du sol. Basé sur les résultats des essais, la relation entre le tassement de la surface et le nombre de passages du vibro-compacteur pouvait être représentée de manière appropriée par un modèle hyperbolique. Après le compactage, les contours de l'incrément de contrainte verticale $\Delta\sigma_v$ étaient semblables à des cercles concentriques après le premier passage du vibro-compacteur et après 8 passages, et le $\Delta\sigma_v$ diminuait graduellement à partir de la zone centrale de compactage. Les contours de l'incrément de contrainte horizontale $\Delta\sigma_h$ formaient deux zones circulaires de contraintes élevées et $\Delta\sigma_h$ diminuait graduellement à partir de la zone centrale après le premier compactage. Les contours de $\Delta\sigma_h$ étaient semblables à des cercles concentriques après 8 passages du vibro-compacteur. La profondeur de la zone de compaction induite augmentait avec l'accroissement de l'énergie de compactage. Basé sur les résultats des essais, la mécanique des sols du remblai après le premier passage du vibro-compacteur pouvait être simulée à l'aide d'un test de résistance au cisaillement d'une semelle peu profonde. Cependant, après 8 passages du vibro-compacteur, l'interaction entre le compacteur et le sol pouvait alors être simulée par la pénétration d'un pieu carré dans un sol meuble.

Keywords : sand, model test, compaction, settlement, relative density, earth pressure

1 INTRODUCTION

In the construction of highway embankments and earth dams, engineers would compact the loose fill to increase its unit weights. The objective of the compaction operation is to improve the engineering properties of soil such as to increase the bearing capacity or to reduce settlement. Compaction is a particular kind of soil stabilization method and it is one of the oldest methods for improving existing soil or man-placed fills.

To analyze the residual lateral earth pressure induced by soil compaction, several methods of analysis have been proposed by Ingold (1979), Duncan and Seed (1986), Peck and Mesri (1987) and other researchers. However, little information regarding the mechanism of the compacted soil has been reported.

This study simulates the two-dimensional line-compaction with a vibratory compactor on the surface of a loose granular soil in the field. Tests results obtained included the surface settlement, the change of soil density, and the change of stresses in the soil mass due to compaction. Based on the test data, the mechanism of the compacted soil due to the strip compaction on the surface of a sandy soil mass is explored.

2 EXPERIMENTAL APPARATUS

To investigate the effects of vibratory compaction on a cohesionless soil mass, the instrumented non-yielding model retaining wall facility (Chen and Fang, 2002) at National Chiao Tung University (NCTU) was used.

To constitute a plane strain condition for model testing, the soil bin was designed to minimize the lateral deflection of sidewalls and the friction between the backfill and sidewalls. The soil bin was fabricated of steel plates with inside dimensions of 1500 mm x 1500 mm x 1600 mm as shown in Figure 1. To minimize the friction between the backfill and sidewalls, a lubrication layer consisted of plastic sheets was furnished for all model wall experiments. The lubrication layer proposed by Fang et al. (2004) consisted of one thick and two thin plastic sheets hung vertically on each sidewall of the soil bin before the backfill was deposited.

To investigate the distribution of stresses in the backfill, a series of soil pressure transducers (Kyowa BE-2KCM17, capacity = 98.1 kN/m^2) were used. The transducers were buried in the soil mass to measure the variation of vertical and horizontal earth pressure during the filling and compaction process.

doi:10.3233/978-1-60750-031-5-700

To simulate the compaction of loose soil in the field, a vibratory compactor was made by attaching an eccentric motor (Mikasa Sangyo, KJ75-2P) to a 0.225 m × 0.225 m steel plate. The total mass of the vibratory compactor was 12.1 kg. The amplitude of downward cyclic vertical force (static + dynamic) measured with a load cell placed under the base plate of the vibratory compactor was 1.767 kN. The measured frequency of vibration was 44 Hz. Assuming the distribution of contact pressure between the base plate and soil was uniform, the downward cyclic normal stress σ_{cyc} applied to the surface of the soil was 34.9 kN/m^2.

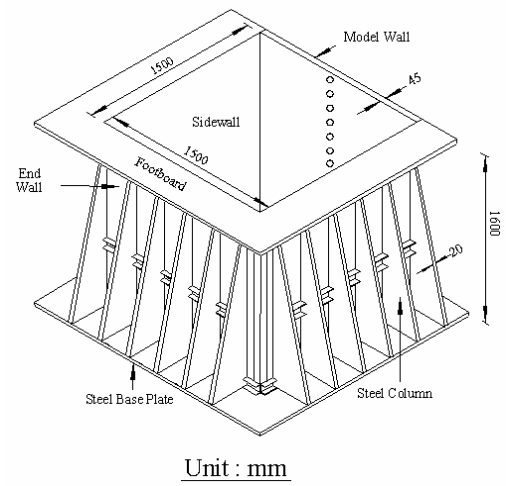

Figure 1. NCTU non-yielding model retaining wall and soil bin.

Air-dry Ottawa sand was used as fill material. To simulate the effects of compaction on the surface of a loose fill, the vibratory compactor was pulled over the compaction lane from the left sidewall to the right sidewall as shown in Figure 2. Then the compactor was turned around 180 degrees to compact the same lane for the second pass. At the end, the fill below the compaction lane had been compacted for eight passes with the compactor. The compaction lane was 0.225 m-wide, 1.5 m-long and each pass took 70 seconds.

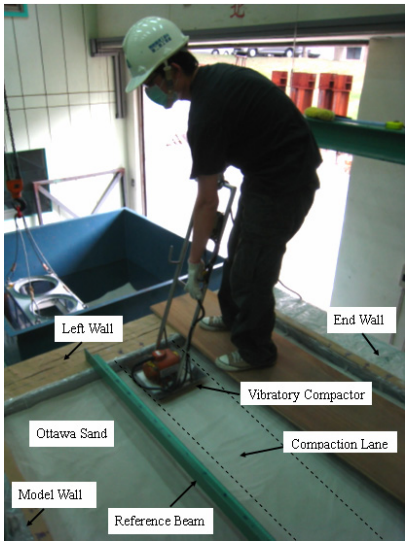

Figure 2. Compaction lane on surface of Ottawa sand.

3 TEST RESULTS

This section reports the variation of the surface settlement, relative density, vertical stress and the horizontal stress due to the strip compaction on the surface of the fill.

Figure 3 shows the surface settlement increased with the increasing number of passes N of the compactor. The surface settlement S shown in Figure 4 was the average settlement of the seven points (point B to H) shown in Figure 3. In Figure 4, the data points obtained from tests 0701 and 0703 indicated that the test results were quite reproducible. Based on the test results, a hyperbolic model was proposed to estimate the surface settlement S as a function of the number of passes of the compactor. The hyperbolic relationship can be expressed as:

$$S = \frac{N}{0.0178 + 0.0241N} \quad (1)$$

where S is the surface settlement in mm, and N is number of passes of the compactor.

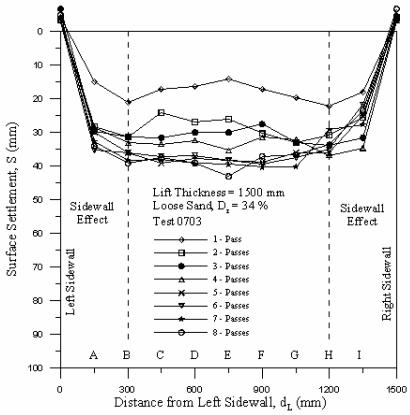

Figure 3. Surface settlement profile of compaction lane.

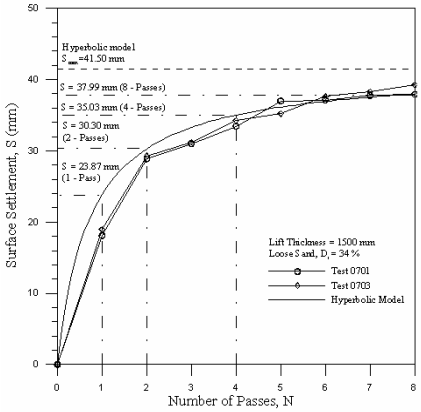

Figure 4. Hyperbolic model to estimate surface settlements S as a function of number of passes of compactor N.

Figure 5 shows the contours of relative density in soil mass after the first passage of the compactor. Before compaction, the fill has a uniform relative density of 34%. Under the compaction lane, the soil density became quite dense (D_r = 64%), and the soil density decreased gradually with the distance from the compaction lane. From the relative density of 34% to 64%, the effects of vibratory compaction on soil density were quite obvious right below the compactor. As the number of passes increased to 8, more compaction energy was transmitted to the soil. In Figure 6, the region of dense sand (D_r = 72%) expanded with the increasing number of the compactor passes. The maximum relative density below the compactor was 75%. The relative density 64% and 75% is corresponding to the dry unit weight 16.3 kN/m^3 and 16.6 kN/m^3, respectively.

In Figure 7, the contours of $\Delta\sigma_v$ after the first passage of the compactor were analogous to a series of concentric circles. The

center of the concentric circles corresponding to the maximum $\Delta\sigma_v$ was located at the depth of 300 mm below the surface. The $\Delta\sigma_v$ would decrease gradually from the central high-stress region.

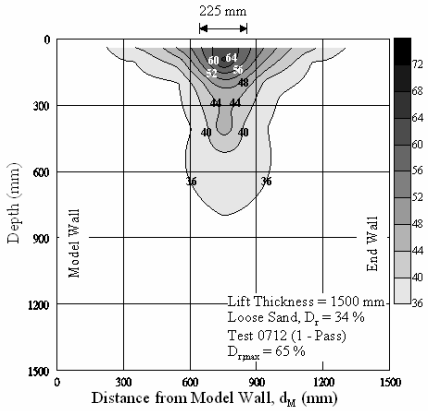

Figure 5. Contours of relative density after 1 – pass of compactor.

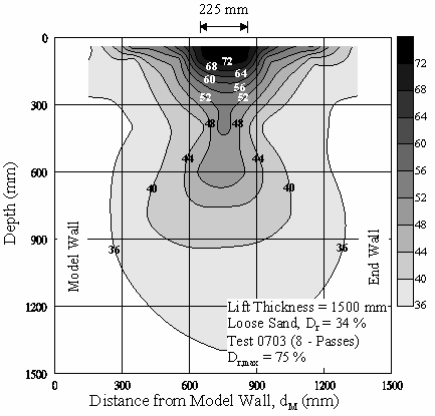

Figure 6. Contours of relative density after 8 – passes of compactor.

Before compaction, vertical stress at the depth of 300 mm calculated by $\sigma_v = \gamma z$ was 4.68 kN/m^2. The incremental vertical stress $\Delta\sigma_v$ was 2.2 kN/m^2 and the incremental stress ratio was 53.0%.

In Figure 6, the relative density of soil changed from the initial value 34% to the maximum value of 72%. At z = 300 mm, the vertical stress increment due to the change of γ (from 15.6 kN/m^3 to 16.6 kN/m^3) was 0.30 kN/m^2. The Comparison between 2.2 kN/m^2 and 0.30 kN/m^2, indicated that the vertical stress increment $\Delta\sigma_v$ was not only affected by the change of soil unit weight. The change of vertical stress was related to the compaction-induced stresses.

It may be concluded that the compaction-induced vertical stresses were quite significant below the compaction lane. As the number of passes increased to 8, more compaction energy was input into the soil mass. In Figure 8, the contours showed that the depth of the compaction-induced zone increased with increasing energy input. The vertical stress increment $\Delta\sigma_v$ increased with increasing number of passage of the compactor.

In Figure 9, the contours of $\Delta\sigma_h$ formed two regions of stress concentration at the depth of 300 mm below the surface. Below the peak-stress points, $\Delta\sigma_h$ gradually decreased with increasing depth. At z = 300mm, the initial horizontal stress calculated by Jaky's equation was 2.27 kN/m^2. The incremental horizontal stress $\Delta\sigma_h$ was up to 1.40 kN/m^2 and the stress incremental ratio was 62 %. It may be concluded that the compaction-induced horizontal stresses were quite obvious below the compaction lane.

However, as the number of passes of the compactor increased to 8, the double high-stress regions merged, and the contours of $\Delta\sigma_h$ were analogous to a series of concentric circles as shown in Figure 10. It is clear in figures 9 and 10 that the depth of the compaction-influenced zone increased with increasing compaction energy input.

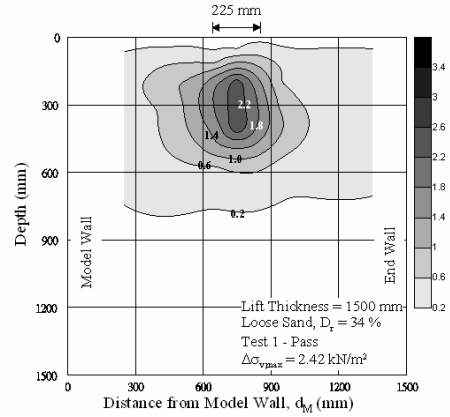

Figure 7. Contours of $\Delta\sigma_v$ after 1 – pass of compactor.

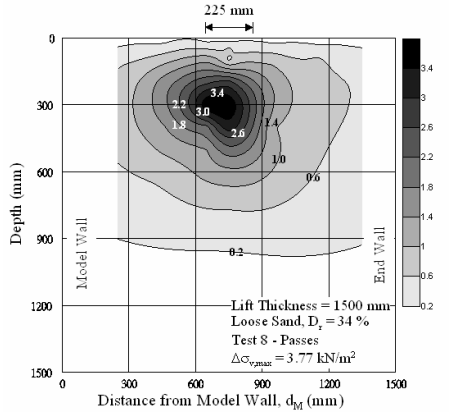

Figure 8. Contours of $\Delta\sigma_v$ after 8 – passes of compactor.

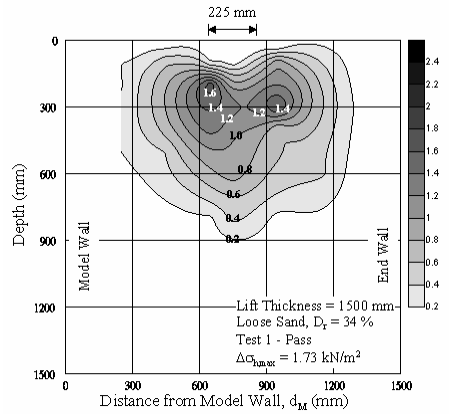

Figure 9. Contours of $\Delta\sigma_h$ after 1 – pass of compactor.

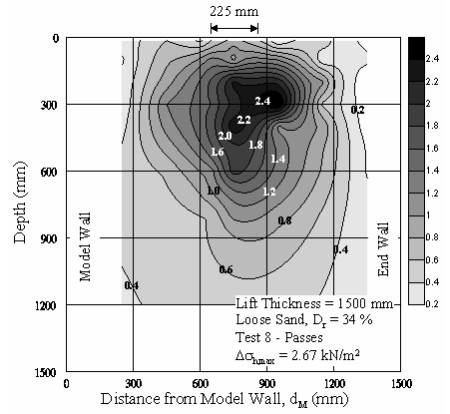

Figure 10. Contours of $\Delta\sigma_h$ after 8 – passes of compactor.

4 MECHANISM OF SOILS UNDER STRIP COMPACTION

Based on the test results reported in previous sections, the mechanism of soils under strip compaction is discussed in this section.

Based on the contours of $\Delta\sigma_h$ in the soil mass after the first passage of the compactor shown in Figure 9, Figure 11 shows the comparison between contours of $\Delta\sigma_h$ in this study and soils under the bearing capacity failure mode (Vesic, 1973). The horizontal stresses under the compactor did not increase which was analogous to the elastic zone under the footing. In Vesic's model, soils in the radial shear zones were pushed by the downward penetration of the footing. In Figure 11, the two high stress zones were thus induced. The mechanism of soils after the first pass of the compactor could be properly explained by local-shear bearing capacity failure mode.

Based on the study of Yang (2006) shown in Figure 12, the influenced range below the pile tip in clean sand would be 3.5D ~ 5.5D, where D is pile diameter. Calculating the influenced zone of compaction by substituting the compactor width B = 225 mm for D, the influence range would be 788 mm ~ 1238 mm. In figure 8 and figure 10, the depth of influence zone for $\Delta\sigma_v$ and $\Delta\sigma_h$ was 800 mm ~ 1200 mm, respectively.

Figure 12 shows both the contours of $\Delta\sigma_h$ measured after 8 passes of the compactor and the influenced zone for a single pile driven in cohesionless soil (Yang, 2006). The influenced zone of compaction is analogous to the stresses below the tip of the pile in cohesionless soil. The mechanism of soils after 8 passes of the compactor could be simulated by a single pile driven in a cohesionless soil.

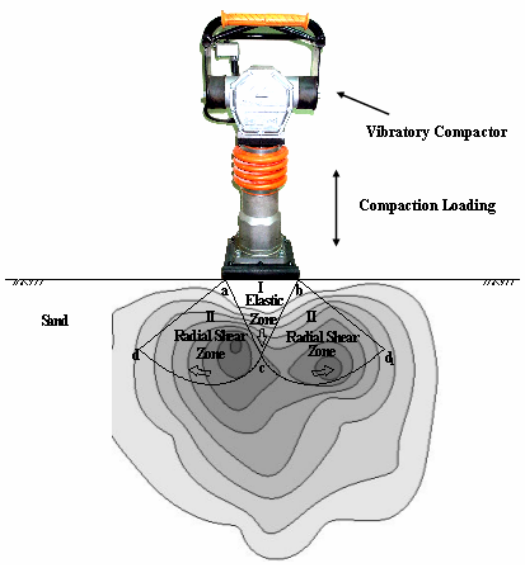

Figure 11. Comparison between horizontal stress increase and local shear failure. (redrawn after Vesic, 1973)

5 CONCLUSIONS

In this study, the effects of strip compaction on sand are investigated. Based on the test results, the following conclusions can be drawn.

1. The surface settlement increased with the increasing number of passes of the compactor. The relationship between the surface settlement and the number of passes of the compactor could be properly described by the hyperbolic model.
2. The contours of $\Delta\sigma_v$ after the first passage of the compactor were analogous to a series of concentric circles. As the number of passes increased to 8, more compaction energy was input to the soil mass and the depth of the compaction-induced zone increased with increasing energy input.

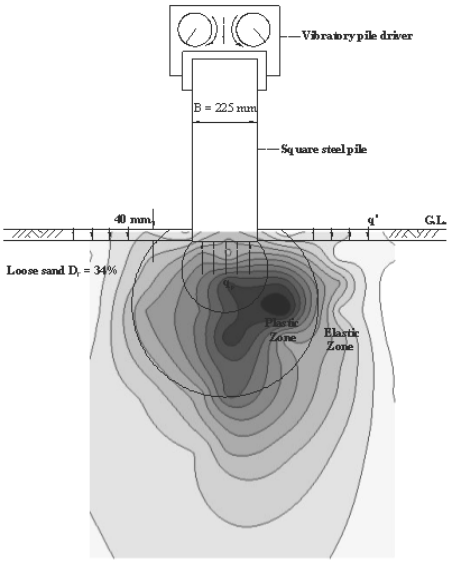

Figure 12. Comparison between test results and influenced zone for a pile driven into sand. (redrawn after Yang, 2006)

3. After the first pass of the compactor, the contours of $\Delta\sigma_h$ formed two regions of stress concentration at the depth of 300 mm below the surface. As the number of passage of the compactor increased to 8, the two high-stress regions merged.
4. The mechanism of soils after the first passage of the compactor could be properly explained by local-shear bearing capacity failure mode. The mechanism of soils after 8 passes of the compactor could be simulated by a single pile driven into a cohesionless soil.

ACKNOWLEDGEMENTS

The writers wish to acknowledge the National Science Council of the Republic China government Grant No. (NSC 95-2221-E-009-199) for the financial assistance that made this investigation possible.

REFERENCES

Chen, T. J., & Fang, Y. S. 2002. A new facility for measurement of earth pressure at-rest. *Geotechnical Engineering Journal*, 3(12): 153-159.

Duncan, J. M., & Seed, R. B. 1986. Compaction-induced earth pressures under K_o-conditions. *Journal of Geotechnical Engineering*, 112(1): 1-22.

Fang, Y. S., Chen, T. J., Holtz, R. D., & Lee, W. F. 2004. Reduction of boundary friction in model tests. *Geotechnical Testing Journal*, 27(1): 1-10.

Ingold, T. S. 1979. The effects of compaction on retaining walls. *Geotechnique*, 19(3): 265-283.

Peck, R. B. & Mesri, G. 1987. Discussion of Compaction-induced earth pressures under K_o-conditions. *Journal of Geotechnical Engineering*, 113(11): 1406-1408.

Vesic, A. S. 1973. Analysis of ultimate loads of shallow foundations. *Journal of the Soil Mechanics and Foundations Division*, 99(SM1): 45-73.

Yang, J. 2006. Influence zone for end bearing of piles in sand. *Journal of Geotechnical & Geoenvironmental Engineering*, 132(9): 1229-1237.

行政院國家科學委員會補助參與國際學術會議報告

專題研究計畫補助編號：NSC 98-2221-E-009-135 及 NSC 97-2221-E-009-124

報告人: 方永壽教授
服務機構: 國立交通大學土木工程系所
職稱: 教授

會議名稱: 第 17 屆國際土壤力學及大地工程研討會 (17th International Conference on Soil Mechanics and Geotechnical Engineering)

舉辦地點: Alexandria, Egypt
舉辦時間: 2009 年 10 月 5 日~9 日

主辦單位:

1. International Society of Soil Mechanics and Geotechnical Engineering (ISSMGE)
2. Egyptian Geotechnical Society
3. Government of Egypt
4. City of Alexandria

國科會專題研究計畫補助編號：
NSC 98-2221-E-009-135 及 NSC 97-2221-E-009-124

攜回資料: 研討會論文集 4 大冊及論文集光碟 1 片

一、參加會議經過

國際土壤力學及大地工程研討會 (International Conference on Soil Mechanics and Geotechnical Engineering)是全世界最大、也是最重要的大地工程研討會。這項研討會是由國際土壤力學及基礎工程學會(International Society of Soil Mechanics and Geotechnical Engineering)；埃及大地工程學會(Egyptian Geotechnical Society)；埃及政府(Government of Egypt)；及亞歷山卓市政府(City of Alexandria)共同主辦。本次國際會議有來自 80 餘國家大約 1,200 位代表參與，4 大本論文集共收錄 700 多篇論文。上圖左起為中華民國大地工程學會理事長台科大廖洪鈞教授、計畫主持人方永壽、及中興顧問公司江政恩主任合影於研討會場。

大會於研討會前兩天(2009/10/5 及 2009/10/6)邀請數位知名的大地工程學者發表演講,例如大會於 2009 年 10 月 5 日上午邀請澳洲 Prof. Poulos 進行 Terzaghi Oration 專題演講，介紹中東超高層建築物深基礎面臨的挑戰，大師級學者的報告內容精采，與會者收穫甚為豐富。大會於 2009 年 10 月 5 日下午邀請美國 Georgia Tech.的 Prof. Paul Mayne 進行 State of the Art (SOA #1)專題演講，介紹大地材料行為及試驗(Geomaterial behavior and testing)，報告內容精采，甚具啟發性。下圖左起為交大黃安斌教授、Prof. Paul Mayne、及計畫主持人方永壽於(SOA #1)專題演講後共進午餐時所攝的照片。

本次研討會於研討會後兩天(2009/10/7 及 2009/10/8)，透過下列主題集中的 16 個討論會場次(Parallel Sessions)，由 General Reporter, Panelists 及 Selected Authors 發表經詳細審查、具重要性的論文，進行國際水準的論文發表，促進學術界與工業界的跨領域交流。

1A - Laboratory Testing
1B - Physical and Constitutive Modeling
1C - Problematic Soils and Geosynthetic Material
1D - In-situ Testing
2A - Deep Foundations & Retaining Walls
2B - Slopes and Embankments
2C - Underground Structures
3A - Instrumentation in Geotechnical Engineering
3B - Monitoring and Performance
3C - Interactive Design
4A - Ground Improvement, Grouting and Dredging
4B - Deep Excavation, Tunneling and Groundwater Control
4C - Natural Hazard Mitigation
5A - Owner, Engineer and Contractor Public Awareness
5B - Management of Geotechnical Data and Processes
5C - Training of Geotechnical Engineers/Future of Geotechnical Engineering Education

二、論文刊出

報告人及研究生簡煜倫合著之論文"Variation of soil density and earth pressure due to strip compaction"，被編列在研討會主題 1B (Physical and Constitutive Modeling)，論文被發表在研討會論文集第一冊、第 700 至 704 頁。此項研究依據實驗方法探討條型夯實振動造成砂土密度及土壓力之變化，為國科會專題研究計畫 NSC 95-2211-E-009-199 之研究成果。

三、考察參觀心得

同行參與此項研討會的國內學者包含交通大學黃安斌教授、台灣大學翁作新教授、陳正興教授、林美聆教授、台科大廖洪鈞教授、李維峰博士、中原大學馮道偉教授、淡江大學張德文教授及中興顧問公司江政恩主任等。

3-1 各國代表參加人數

大會公佈至 2009 年 9 月 30 日為止，已註冊報名參加研討會的各國代表名單(List of participants)，總共有來自 81 個國家、大約 1,200 位代表與會，其中代表人數列前 20 名的國家名稱及代表人數如下表所列：

名次	國家名稱(參加人數)	名次	國家名稱(參加人數)
1	Japan (101)	11	Netherlands (27)
2	United States (55)	12	Korea (24)
3	Egypt (53)	13	Canada (21)
4	China (47)	14	Spain (17)
5	France (38)	15	United Kingdom (16)
6	Germany (36)	16	India (16)
7	Australia (35)	17	Greece (15)
8	Italy (34)	18	Taiwan (12)
9	Brazil (31)	19	Hong Kong (12)
10	Russia (27)	20	Turkey (12)

日本是上一屆 16th ICSMGE 的主辦國，埃及是本屆 17th ICSMGE 的主辦國，所以日本與埃及代表人數特別龐大。美國、法國、德國、澳洲及義大利是傳統工程強國，大地工程人才濟濟，所以與會代表特別多。我國註冊出席代表 12 人，大致與我國人口成合理比例。上表中排名第 4 的 China，近年經濟及工程發展有長足的進步，由其代表團人數可以看出其逐步跨入國際舞台之趨勢。

3-2 音樂裊繞的開幕典禮

開幕典禮乃是研討會枯燥乏味又必要的儀式，在 2009 年 10 月 5 日上午的開幕典禮中，埃及政府長官、亞歷山卓市政府長官、國際大地工程學會會長 Prof. Pinto、及 17th ICSMGE 研討會主辦人 Prof. Hamza 依序上台官式致詞。

在長官致詞告一段落後，舞台布幕緩緩升起，舞台上出現一個大約 20 人的弦樂團，如下圖所示。隨著飛舞的指揮棒，他們流暢的奏出具埃及風味的美妙音樂，各國代表心中頓時感覺輕鬆愉快，暫時忘卻無聊的官

式致詞，放下國界與文化藩籬，融入一片愉悅的旋律，這份別出心裁的安排，受到與會者一致的好評。

Variation of soil density and earth pressure due to strip compaction

Variation de la densité et de la poussée du sol due à un compactage en bande

Y.S. Fang
Department of Civil Engineering, National Chiao Tung University, Hsinchu, Taiwan
Y.L. Chien
Power Projects, Civil Dept., E & C Corporation, Taipei, Taiwan

ABSTRACT

This paper studies the variation of soil density and earth pressure in a soil mass due to the vibratory compaction along a strip on the surface of the cohesionless backfill. Experiments were conducted in a non-yielding model retaining wall facility and dry Ottawa sand was used as fill material. Based on the test results, it is found that surface settlement increased with the increasing number of passage of the compactor. The relationship between the surface settlement and the number of passes could be properly described by the hyperbolic model. The contours of $\Delta\sigma_v$ after the first passage of the compactor were analogous to a series of concentric circles. As the number of passes increased to 8, the depth of the compaction-induced zone increased with increasing energy input. After the first passage of the compactor, the contours of $\Delta\sigma_h$ formed two regions of stress concentration below the surface. As the number of passage increased to 8, the two high-stress regions merged. The mechanism of soils after the first passage of the compactor could be properly explained by local-shear bearing capacity failure mode. The mechanism of soils after 8 passes of the compactor could be simulated by a single pile driven into a cohesionless soil.

RÉSUMÉ

Cet article étudie les variations de la densité et de la poussée du sol après le compactage par vibration d'une bande à la surface d'un remblai meuble. Des expériences furent réalisées pour étudier les effets d'un vibro-compacteur sur la densification du sol. Basé sur les résultats des essais, la relation entre le tassement de la surface et le nombre de passages du vibro-compacteur pouvait être représentée de manière appropriée par un modèle hyperbolique. Après le compactage, les contours de l'incrément de contrainte verticale $\Delta\sigma_v$ étaient semblables à des cercles concentriques après le premier passage du vibro-compacteur et après 8 passages, et le $\Delta\sigma_v$ diminuait graduellement à partir de la zone centrale de compactage. Les contours de l'incrément de contrainte horizontale $\Delta\sigma_h$ formaient deux zones circulaires de contraintes élevées et $\Delta\sigma_h$ diminuait graduellement à partir de la zone centrale après le premier compactage. Les contours de $\Delta\sigma_h$ étaient semblables à des cercles concentriques après 8 passages du vibro-compacteur. La profondeur de la zone de compaction induite augmentait avec l'accroissement de l'énergie de compactage. Basé sur les résultats des essais, la mécanique des sols du remblai après le premier passage du vibro-compacteur pouvait être simulée à l'aide d'un test de résistance au cisaillement d'une semelle peu profonde. Cependant, après 8 passages du vibro-compacteur, l'interaction entre le compacteur et le sol pouvait alors être simulée par la pénétration d'un pieu carré dans un sol meuble.

Keywords : sand, model test, compaction, settlement, relative density, earth pressure

1 INTRODUCTION

In the construction of highway embankments and earth dams, engineers would compact the loose fill to increase its unit weights. The objective of the compaction operation is to improve the engineering properties of soil such as to increase the bearing capacity or to reduce settlement. Compaction is a particular kind of soil stabilization method and it is one of the oldest methods for improving existing soil or man-placed fills.

To analyze the residual lateral earth pressure induced by soil compaction, several methods of analysis have been proposed by Ingold (1979), Duncan and Seed (1986), Peck and Mesri (1987) and other researchers. However, little information regarding the mechanism of the compacted soil has been reported.

This study simulates the two-dimensional line-compaction with a vibratory compactor on the surface of a loose granular soil in the field. Tests results obtained included the surface settlement, the change of soil density, and the change of stresses in the soil mass due to compaction. Based on the test data, the mechanism of the compacted soil due to the strip compaction on the surface of a sandy soil mass is explored.

2 EXPERIMENTAL APPARATUS

To investigate the effects of vibratory compaction on a cohesionless soil mass, the instrumented non-yielding model retaining wall facility (Chen and Fang, 2002) at National Chiao Tung University (NCTU) was used.

To constitute a plane strain condition for model testing, the soil bin was designed to minimize the lateral deflection of sidewalls and the friction between the backfill and sidewalls. The soil bin was fabricated of steel plates with inside dimensions of 1500 mm x 1500 mm x 1600 mm as shown in Figure 1. To minimize the friction between the backfill and sidewalls, a lubrication layer consisted of plastic sheets was furnished for all model wall experiments. The lubrication layer proposed by Fang et al. (2004) consisted of one thick and two thin plastic sheets hung vertically on each sidewall of the soil bin before the backfill was deposited.

To investigate the distribution of stresses in the backfill, a series of soil pressure transducers (Kyowa BE-2KCM17, capacity = 98.1 kN/m^2) were used. The transducers were buried in the soil mass to measure the variation of vertical and horizontal earth pressure during the filling and compaction process.

doi:10.3233/978-1-60750-031-5-700

To simulate the compaction of loose soil in the field, a vibratory compactor was made by attaching an eccentric motor (Mikasa Sangyo, KJ75-2P) to a 0.225 m × 0.225 m steel plate. The total mass of the vibratory compactor was 12.1 kg. The amplitude of downward cyclic vertical force (static + dynamic) measured with a load cell placed under the base plate of the vibratory compactor was 1.767 kN. The measured frequency of vibration was 44 Hz. Assuming the distribution of contact pressure between the base plate and soil was uniform, the downward cyclic normal stress σ_{cyc} applied to the surface of the soil was 34.9 kN/m^2.

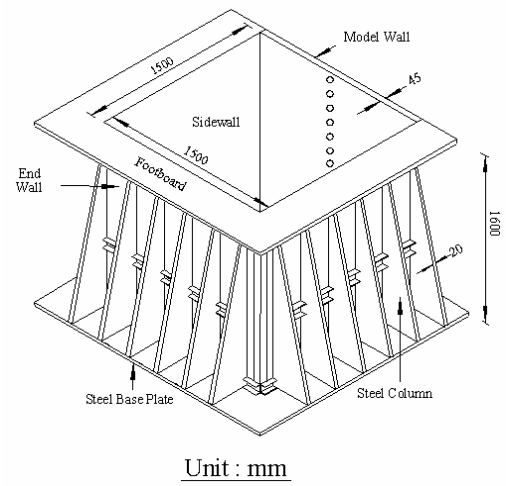

Figure 1. NCTU non-yielding model retaining wall and soil bin.

Air-dry Ottawa sand was used as fill material. To simulate the effects of compaction on the surface of a loose fill, the vibratory compactor was pulled over the compaction lane from the left sidewall to the right sidewall as shown in Figure 2. Then the compactor was turned around 180 degrees to compact the same lane for the second pass. At the end, the fill below the compaction lane had been compacted for eight passes with the compactor. The compaction lane was 0.225 m-wide, 1.5 m-long and each pass took 70 seconds.

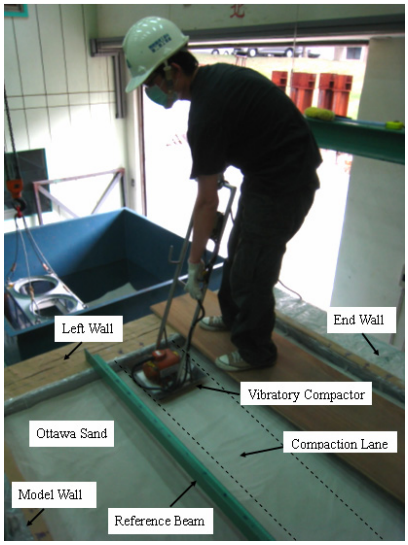

Figure 2. Compaction lane on surface of Ottawa sand.

3 TEST RESULTS

This section reports the variation of the surface settlement, relative density, vertical stress and the horizontal stress due to the strip compaction on the surface of the fill.

Figure 3 shows the surface settlement increased with the increasing number of passes N of the compactor. The surface settlement S shown in Figure 4 was the average settlement of the seven points (point B to H) shown in Figure 3. In Figure 4, the data points obtained from tests 0701 and 0703 indicated that the test results were quite reproducible. Based on the test results, a hyperbolic model was proposed to estimate the surface settlement S as a function of the number of passes of the compactor. The hyperbolic relationship can be expressed as:

$$S = \frac{N}{0.0178 + 0.0241N} \quad (1)$$

where S is the surface settlement in mm, and N is number of passes of the compactor.

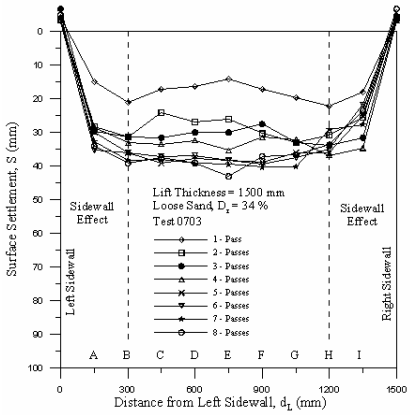

Figure 3. Surface settlement profile of compaction lane.

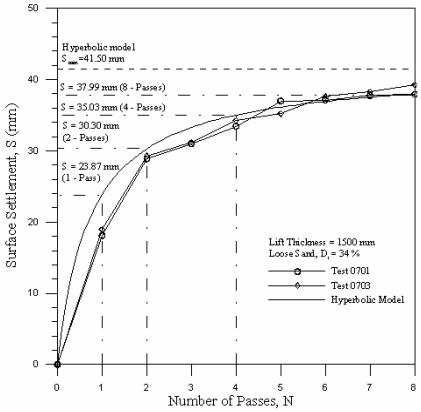

Figure 4. Hyperbolic model to estimate surface settlements S as a function of number of passes of compactor N.

Figure 5 shows the contours of relative density in soil mass after the first passage of the compactor. Before compaction, the fill has a uniform relative density of 34%. Under the compaction lane, the soil density became quite dense (D_r = 64%), and the soil density decreased gradually with the distance from the compaction lane. From the relative density of 34% to 64%, the effects of vibratory compaction on soil density were quite obvious right below the compactor. As the number of passes increased to 8, more compaction energy was transmitted to the soil. In Figure 6, the region of dense sand (D_r = 72%) expanded with the increasing number of the compactor passes. The maximum relative density below the compactor was 75%. The relative density 64% and 75% is corresponding to the dry unit weight 16.3 kN/m^3 and 16.6 kN/m^3, respectively.

In Figure 7, the contours of $\Delta\sigma_v$ after the first passage of the compactor were analogous to a series of concentric circles. The

center of the concentric circles corresponding to the maximum $\Delta\sigma_v$ was located at the depth of 300 mm below the surface. The $\Delta\sigma_v$ would decrease gradually from the central high-stress region.

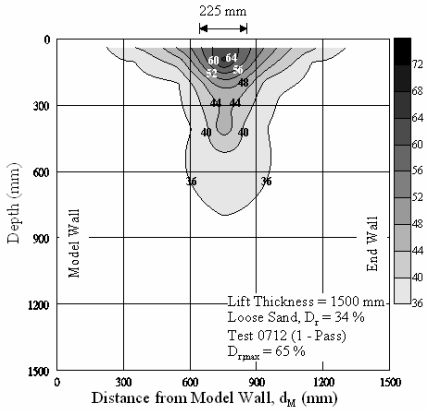

Figure 5. Contours of relative density after 1 – pass of compactor.

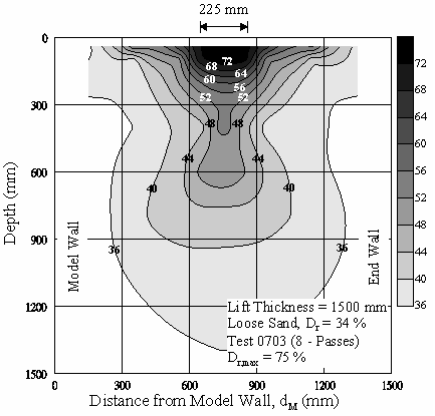

Figure 6. Contours of relative density after 8 – passes of compactor.

Before compaction, vertical stress at the depth of 300 mm calculated by $\sigma_v = \gamma z$ was 4.68 kN/m^2. The incremental vertical stress $\Delta\sigma_v$ was 2.2 kN/m^2 and the incremental stress ratio was 53.0%.

In Figure 6, the relative density of soil changed from the initial value 34% to the maximum value of 72%. At z = 300 mm, the vertical stress increment due to the change of γ (from 15.6 kN/m^3 to 16.6 kN/m^3) was 0.30 kN/m^2. The Comparison between 2.2 kN/m^2 and 0.30 kN/m^2, indicated that the vertical stress increment $\Delta\sigma_v$ was not only affected by the change of soil unit weight. The change of vertical stress was related to the compaction-induced stresses.

It may be concluded that the compaction-induced vertical stresses were quite significant below the compaction lane. As the number of passes increased to 8, more compaction energy was input into the soil mass. In Figure 8, the contours showed that the depth of the compaction-induced zone increased with increasing energy input. The vertical stress increment $\Delta\sigma_v$ increased with increasing number of passage of the compactor.

In Figure 9, the contours of $\Delta\sigma_h$ formed two regions of stress concentration at the depth of 300 mm below the surface. Below the peak-stress points, $\Delta\sigma_h$ gradually decreased with increasing depth. At z = 300mm, the initial horizontal stress calculated by Jaky's equation was 2.27 kN/m^2. The incremental horizontal stress $\Delta\sigma_h$ was up to 1.40 kN/m^2 and the stress incremental ratio was 62 %. It may be concluded that the compaction-induced horizontal stresses were quite obvious below the compaction lane.

However, as the number of passes of the compactor increased to 8, the double high-stress regions merged, and the contours of $\Delta\sigma_h$ were analogous to a series of concentric circles as shown in Figure 10. It is clear in figures 9 and 10 that the depth of the compaction-influenced zone increased with increasing compaction energy input.

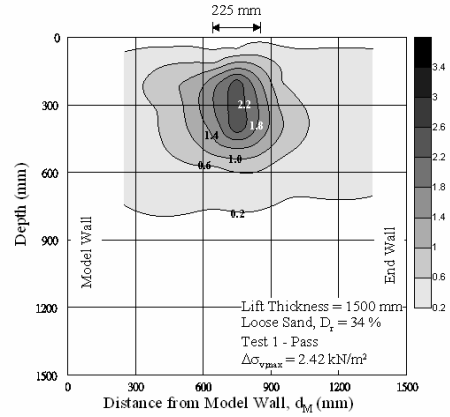

Figure 7. Contours of $\Delta\sigma_v$ after 1 – pass of compactor.

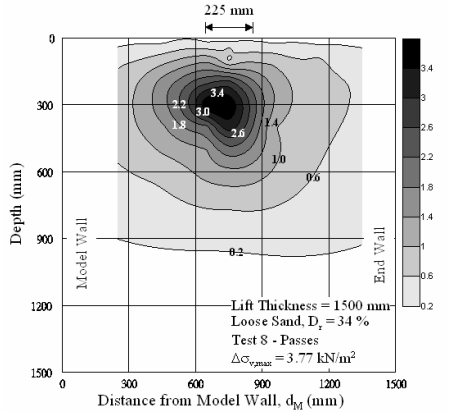

Figure 8. Contours of $\Delta\sigma_v$ after 8 – passes of compactor.

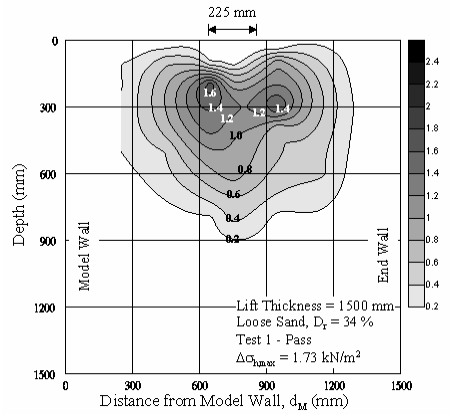

Figure 9. Contours of $\Delta\sigma_h$ after 1 – pass of compactor.

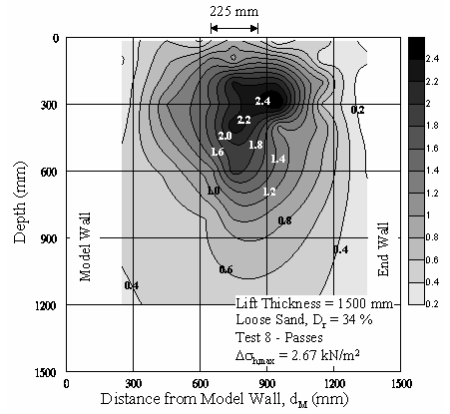

Figure 10. Contours of $\Delta\sigma_h$ after 8 – passes of compactor.

4 MECHANISM OF SOILS UNDER STRIP COMPACTION

Based on the test results reported in previous sections, the mechanism of soils under strip compaction is discussed in this section.

Based on the contours of $\Delta\sigma_h$ in the soil mass after the first passage of the compactor shown in Figure 9, Figure 11 shows the comparison between contours of $\Delta\sigma_h$ in this study and soils under the bearing capacity failure mode (Vesic, 1973). The horizontal stresses under the compactor did not increase which was analogous to the elastic zone under the footing. In Vesic's model, soils in the radial shear zones were pushed by the downward penetration of the footing. In Figure 11, the two high stress zones were thus induced. The mechanism of soils after the first pass of the compactor could be properly explained by local-shear bearing capacity failure mode.

Based on the study of Yang (2006) shown in Figure 12, the influenced range below the pile tip in clean sand would be 3.5D ~ 5.5D, where D is pile diameter. Calculating the influenced zone of compaction by substituting the compactor width B = 225 mm for D, the influence range would be 788 mm ~ 1238 mm. In figure 8 and figure 10, the depth of influence zone for $\Delta\sigma_v$ and $\Delta\sigma_h$ was 800 mm ~ 1200 mm, respectively.

Figure 12 shows both the contours of $\Delta\sigma_h$ measured after 8 passes of the compactor and the influenced zone for a single pile driven in cohesionless soil (Yang, 2006). The influenced zone of compaction is analogous to the stresses below the tip of the pile in cohesionless soil. The mechanism of soils after 8 passes of the compactor could be simulated by a single pile driven in a cohesionless soil.

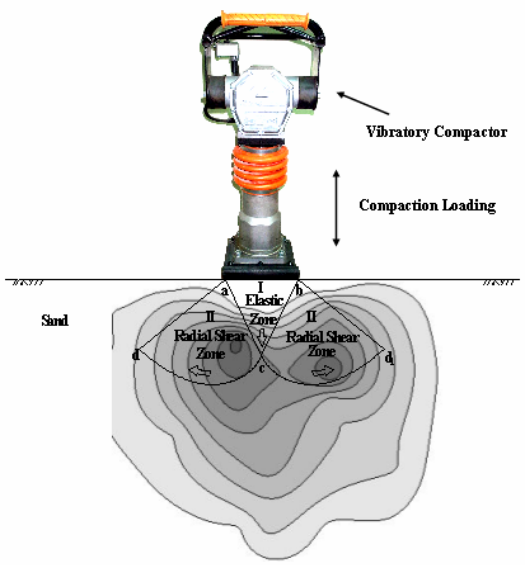

Figure 11. Comparison between horizontal stress increase and local shear failure. (redrawn after Vesic, 1973)

5 CONCLUSIONS

In this study, the effects of strip compaction on sand are investigated. Based on the test results, the following conclusions can be drawn.

1. The surface settlement increased with the increasing number of passes of the compactor. The relationship between the surface settlement and the number of passes of the compactor could be properly described by the hyperbolic model.
2. The contours of $\Delta\sigma_v$ after the first passage of the compactor were analogous to a series of concentric circles. As the number of passes increased to 8, more compaction energy was input to the soil mass and the depth of the compaction-induced zone increased with increasing energy input.

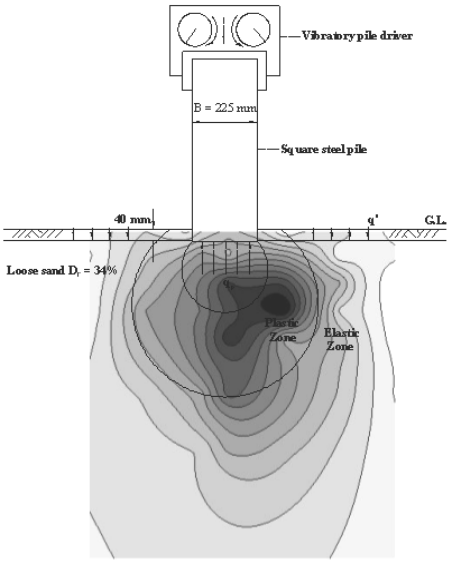

Figure 12. Comparison between test results and influenced zone for a pile driven into sand. (redrawn after Yang, 2006)

3. After the first pass of the compactor, the contours of $\Delta\sigma_h$ formed two regions of stress concentration at the depth of 300 mm below the surface. As the number of passage of the compactor increased to 8, the two high-stress regions merged.
4. The mechanism of soils after the first passage of the compactor could be properly explained by local-shear bearing capacity failure mode. The mechanism of soils after 8 passes of the compactor could be simulated by a single pile driven into a cohesionless soil.

ACKNOWLEDGEMENTS

The writers wish to acknowledge the National Science Council of the Republic China government Grant No. (NSC 95-2221-E-009-199) for the financial assistance that made this investigation possible.

REFERENCES

Chen, T. J., & Fang, Y. S. 2002. A new facility for measurement of earth pressure at-rest. *Geotechnical Engineering Journal*, 3(12): 153-159.

Duncan, J. M., & Seed, R. B. 1986. Compaction-induced earth pressures under K_o-conditions. *Journal of Geotechnical Engineering*, 112(1): 1-22.

Fang, Y. S., Chen, T. J., Holtz, R. D., & Lee, W. F. 2004. Reduction of boundary friction in model tests. *Geotechnical Testing Journal*, 27(1): 1-10.

Ingold, T. S. 1979. The effects of compaction on retaining walls. *Geotechnique*, 19(3): 265-283.

Peck, R. B. & Mesri, G. 1987. Discussion of Compaction-induced earth pressures under K_o-conditions. *Journal of Geotechnical Engineering*, 113(11): 1406-1408.

Vesic, A. S. 1973. Analysis of ultimate loads of shallow foundations. *Journal of the Soil Mechanics and Foundations Division*, 99(SM1): 45-73.

Yang, J. 2006. Influence zone for end bearing of piles in sand. *Journal of Geotechnical & Geoenvironmental Engineering*, 132(9): 1229-1237.

無研發成果推廣資料

國科會補助專題研究計畫成果報告自評表

請就研究內容與原計畫相符程度、達成預期目標情況、研究成果之學術或應用價值（簡要敘述成果所代表之意義、價值、影響或進一步發展之可能性）、是否適合在學術期刊發表或申請專利、主要發現或其他有關價值等，作一綜合評估。

1. 請就研究內容與原計畫相符程度、達成預期目標情況作一綜合評估

■達成目標

□未達成目標（請說明，以 100 字為限）

□實驗失敗

□因故實驗中斷

□其他原因

說明：

2. 研究成果在學術期刊發表或申請專利等情形：

論文：■已發表 □未發表之文稿 □撰寫中 □無

專利：□已獲得 □申請中 ■無

技轉：□已技轉 □洽談中 ■無

其他：(以 100 字為限)

3. 請依學術成就、技術創新、社會影響等方面，評估研究成果之學術或應用價值（簡要敘述成果所代表之意義、價值、影響或進一步發展之可能性）(以 500 字為限)

本研究利用國立交通大學模型擋土牆設備探討震動夯實所引致之土體密度及應力變化。以氣乾渥太華砂作為回填土進行夯實，回填土高 1.5 公尺。回填土初始相對密度為 34%時地表震動夯實對砂土密度與土壓力之影響。本研究獲得數項創新發現，具工程實用價值，上述該研究成果已於 2009 年 10 月於埃及亞歷山卓市(Alexandria, Egypt)舉行的第 17 屆國際土壤力學及大地工程研討會(17th International Conference on Soil Mechanics and Geotechnical Engineering)發表，獲得國際大地工程界肯定，充分達成計劃目標。參與研究的碩士班研究生籍此機會，習得大型基礎模型實驗與資料擷取之操作，以及嚴謹審慎之實驗方法與獨立思考及創造的能力，獲益匪淺。